

# Phase transition induced by magnetic field in a two-leg spin ladder

Takanori Sugimoto,<sup>1,2</sup> M. Mori,<sup>1,2</sup> T. Tohyama,<sup>3</sup> S. Maekawa<sup>1,2</sup>  
ASRC, JAEA,<sup>1</sup> CREST, JST,<sup>2</sup> YITP, Kyoto Univ.<sup>3</sup>

T. Sugimoto, *et al*, PRB 87, 155143 (2013).

# Contents

Model: frustrated two-leg spin ladder

Compound:  $\text{BiCu}_2\text{PO}_6$

Method: Dynamical DMRG

Numerical Results:

Excitation spectrum

Magnetization

Summary

# Model

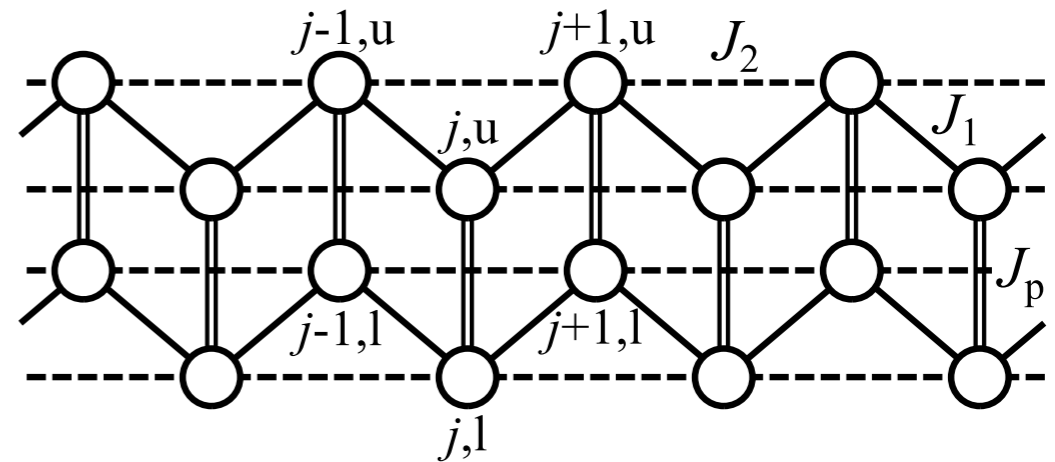
## Frustrated two-leg spin-ladder system

$$\mathcal{H} = \mathcal{H}_1 + \mathcal{H}_2 + \mathcal{H}_p$$

$$\mathcal{H}_1 = J_1 \sum_j \left[ \mathbf{S}_{j,u} \cdot \mathbf{S}_{j+1,u} + \mathbf{S}_{j,l} \cdot \mathbf{S}_{j+1,l} \right]$$

$$\mathcal{H}_2 = J_2 \sum_j \left[ \mathbf{S}_{j,u} \cdot \mathbf{S}_{j+2,u} + \mathbf{S}_{j,l} \cdot \mathbf{S}_{j+2,l} \right]$$

$$\mathcal{H}_p = J_p \sum_j \mathbf{S}_{j,u} \cdot \mathbf{S}_{j,l}$$



# Model

## Frustrated two-leg spin-ladder system

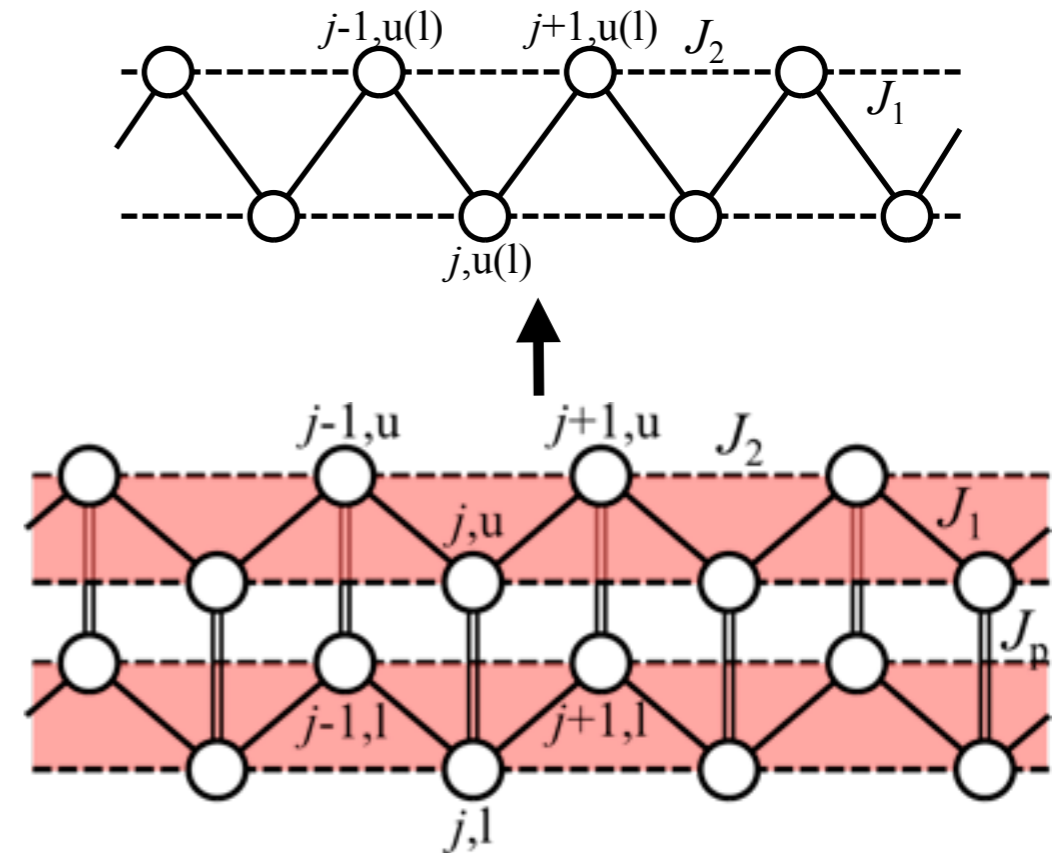
$$\mathcal{H} = \mathcal{H}_1 + \mathcal{H}_2 + \mathcal{H}_p$$

$$\mathcal{H}_1 = J_1 \sum_j \left[ \mathbf{S}_{j,u} \cdot \mathbf{S}_{j+1,u} + \mathbf{S}_{j,l} \cdot \mathbf{S}_{j+1,l} \right]$$

$$\mathcal{H}_2 = J_2 \sum_j \left[ \mathbf{S}_{j,u} \cdot \mathbf{S}_{j+2,u} + \mathbf{S}_{j,l} \cdot \mathbf{S}_{j+2,l} \right]$$

$$\mathcal{H}_p = J_p \sum_j \mathbf{S}_{j,u} \cdot \mathbf{S}_{j,l}$$

## Frustrated spin-chain system





# Model

## Frustrated two-leg spin-ladder system

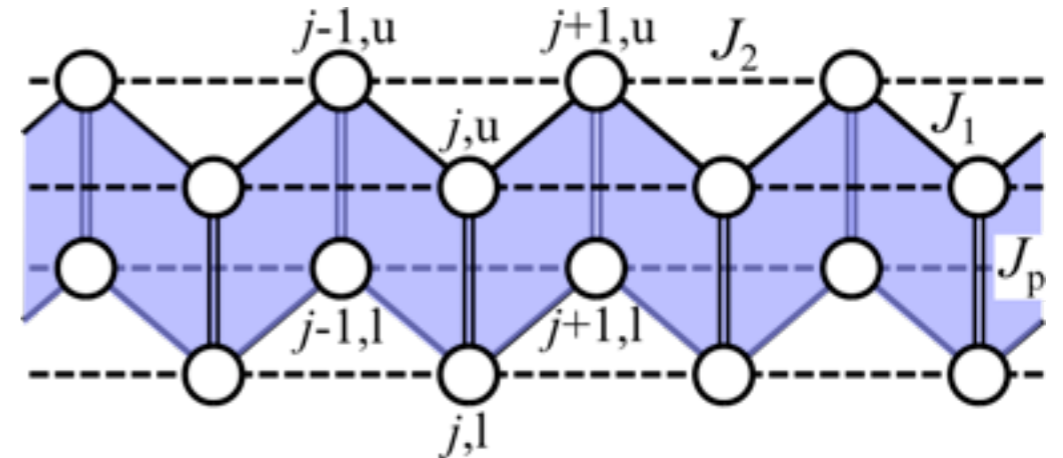
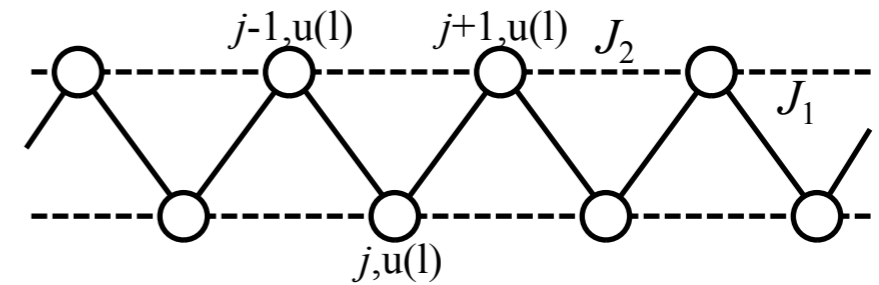
$$\mathcal{H} = \mathcal{H}_1 + \mathcal{H}_2 + \mathcal{H}_p$$

$$\mathcal{H}_1 = J_1 \sum_j \left[ \mathbf{S}_{j,u} \cdot \mathbf{S}_{j+1,u} + \mathbf{S}_{j,l} \cdot \mathbf{S}_{j+1,l} \right]$$

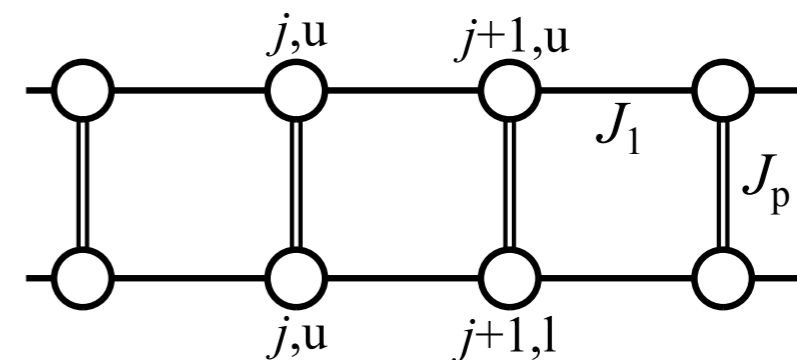
$$\mathcal{H}_2 = J_2 \sum_j \left[ \mathbf{S}_{j,u} \cdot \mathbf{S}_{j+2,u} + \mathbf{S}_{j,l} \cdot \mathbf{S}_{j+2,l} \right]$$

$$\mathcal{H}_p = J_p \sum_j \mathbf{S}_{j,u} \cdot \mathbf{S}_{j,l}$$

## Frustrated spin-chain system



## Non-frustrated spin-ladder system



# Model

## Frustrated two-leg spin-ladder system

$$\mathcal{H} = \mathcal{H}_1 + \mathcal{H}_2 + \mathcal{H}_p$$

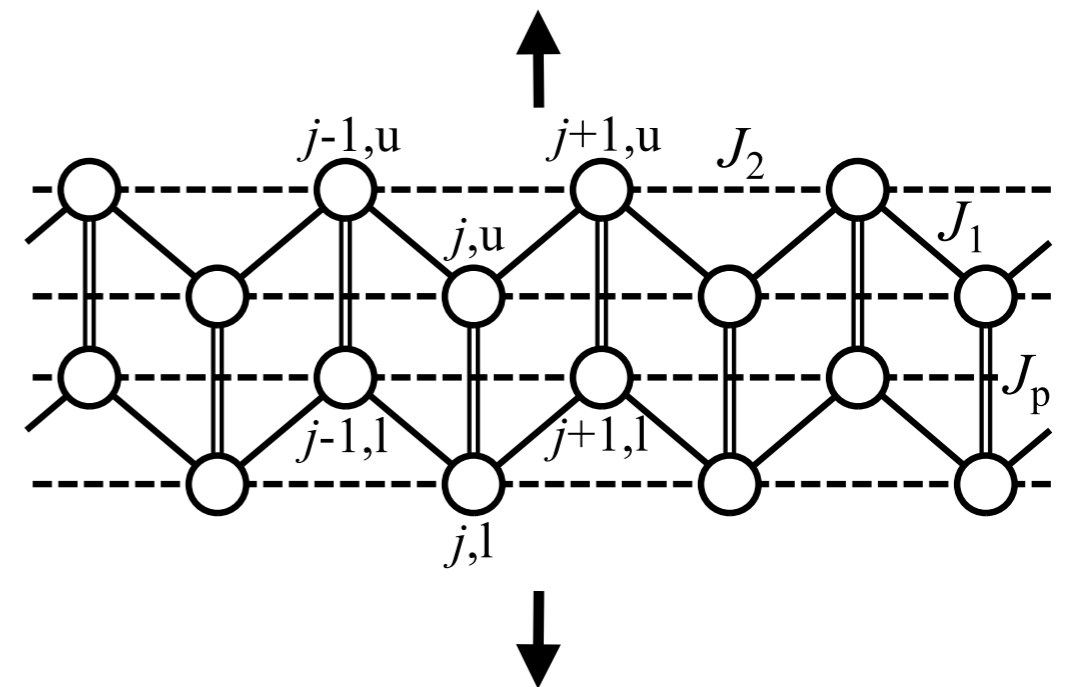
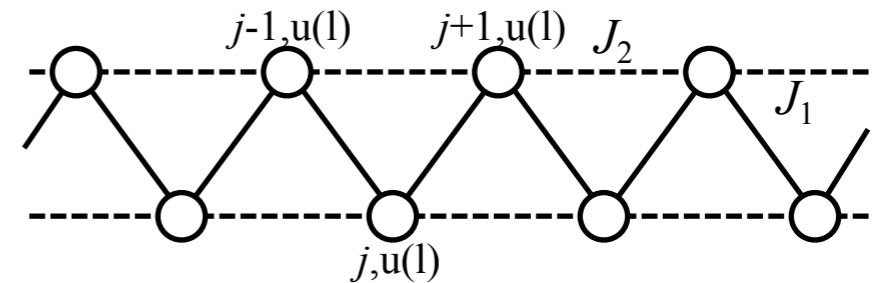
$$\mathcal{H}_1 = J_1 \sum_j \left[ \mathbf{S}_{j,u} \cdot \mathbf{S}_{j+1,u} + \mathbf{S}_{j,l} \cdot \mathbf{S}_{j+1,l} \right]$$

$$\mathcal{H}_2 = J_2 \sum_j \left[ \mathbf{S}_{j,u} \cdot \mathbf{S}_{j+2,u} + \mathbf{S}_{j,l} \cdot \mathbf{S}_{j+2,l} \right]$$

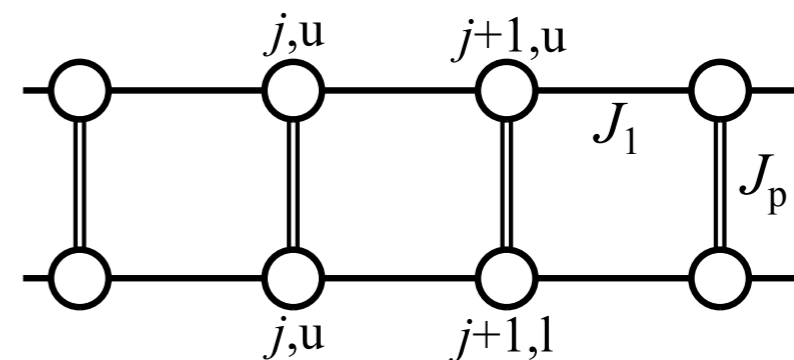
$$\mathcal{H}_p = J_p \sum_j \mathbf{S}_{j,u} \cdot \mathbf{S}_{j,l}$$

➡ This is a bridging model between the frustrated spin chain & non-frustrated spin ladder.

Frustrated spin-chain system ( $J_p=0$ )

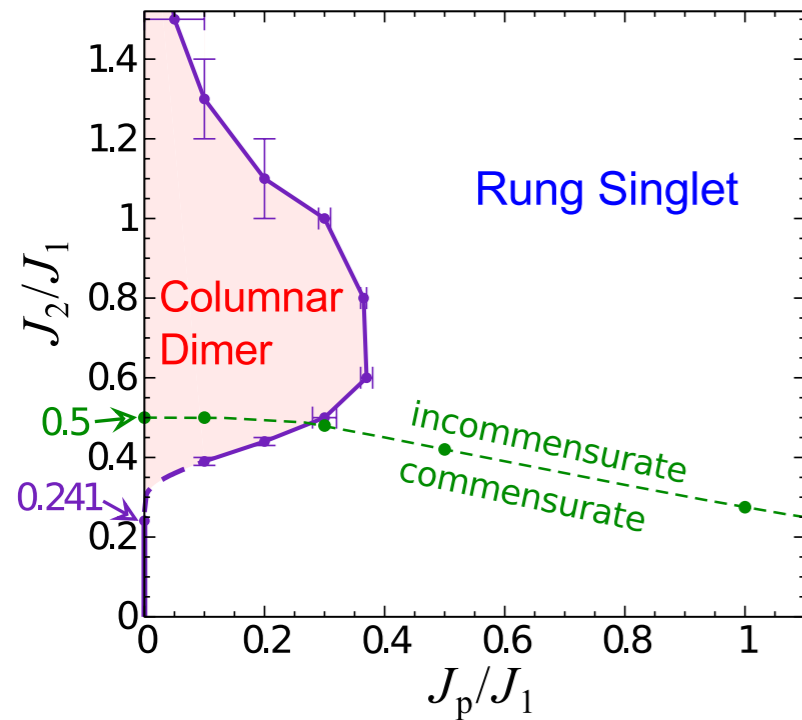


Non-frustrated spin-ladder system ( $J_2=0$ )



# Model

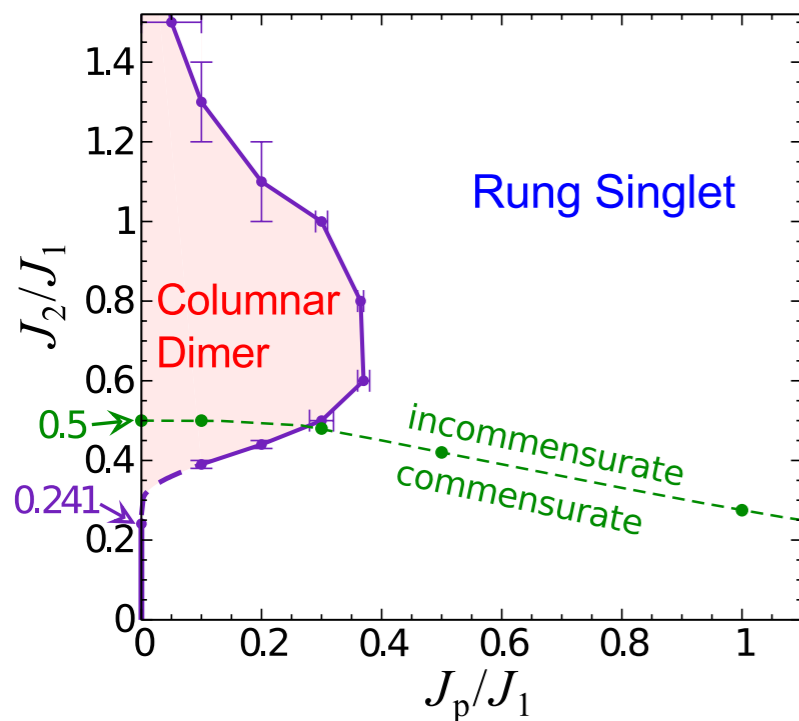
## Ground-state phase diagram



A. Lavarélo, *et al*, PRB 84, 144407 (2011).

# Model

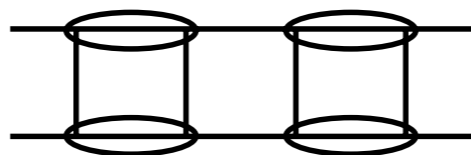
## Ground-state phase diagram



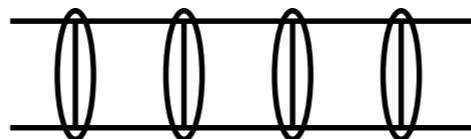
A. Lavaréolo, *et al*, PRB 84, 144407 (2011).

Ground state

Columnar Dimer (CD):



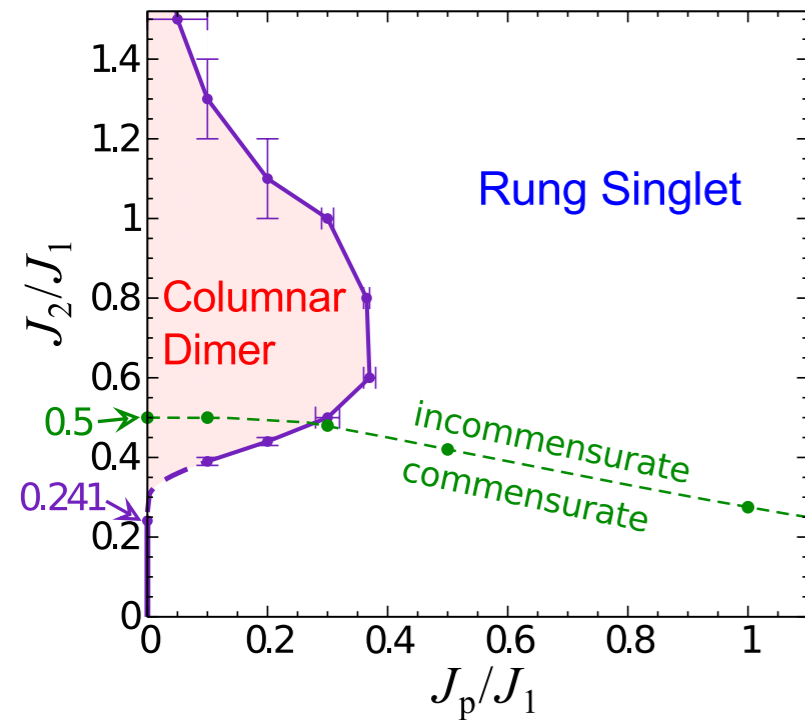
Rung Singlet (RS):



○ : singlet pair

# Model

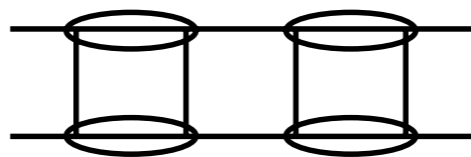
## Ground-state phase diagram



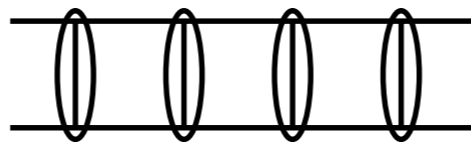
A. Lavaré, *et al*, PRB 84, 144407 (2011).

Ground state

Columnar Dimer (CD):



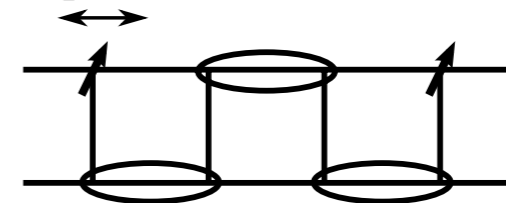
Rung Singlet (RS):



○ : singlet pair

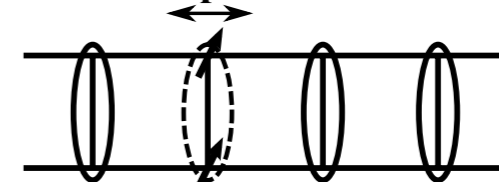
Elementary Excitation

spinon



= Frustrated spin chain

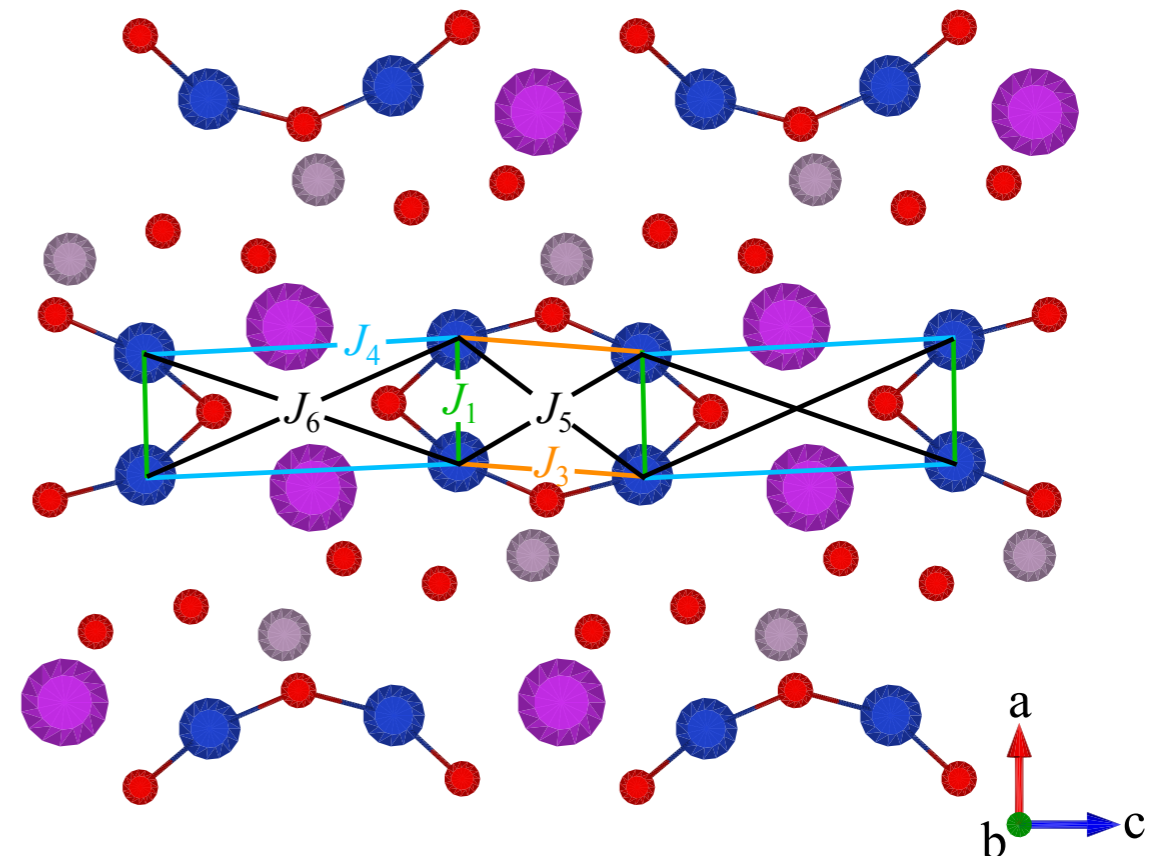
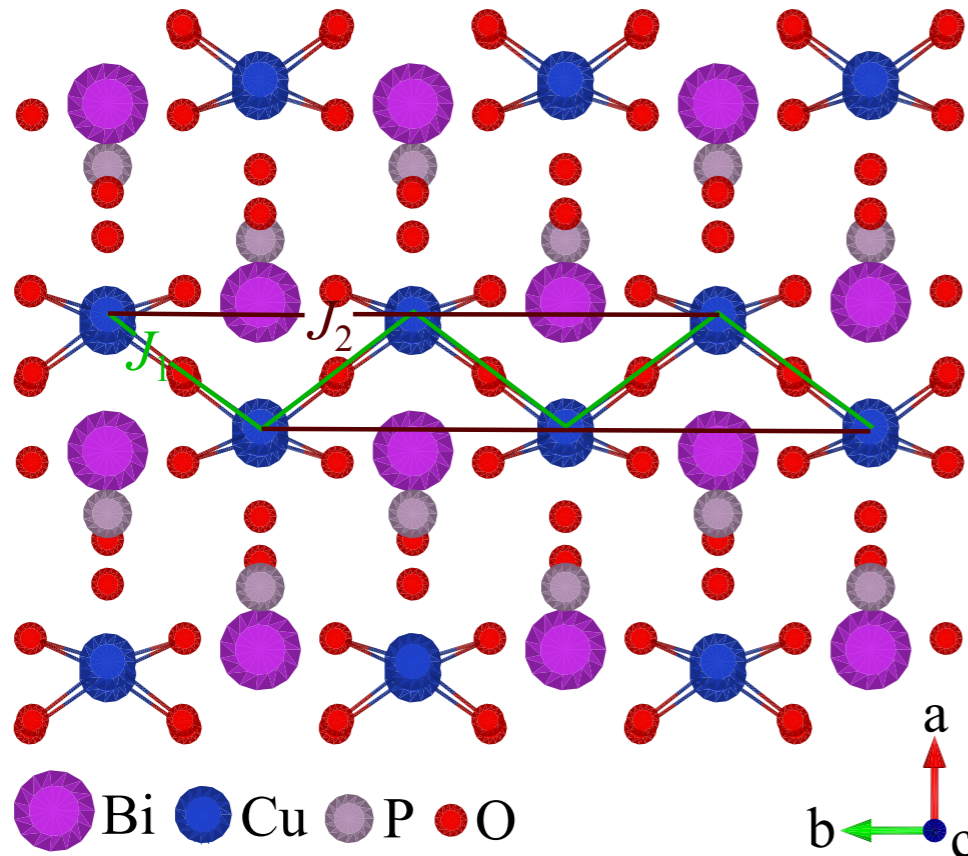
triplon



= Non-frustrated spin ladder

# Real compound

## ◆ Crystal Structure of BiCu<sub>2</sub>PO<sub>6</sub>



## ◆ Exchange energy by DFT calculation

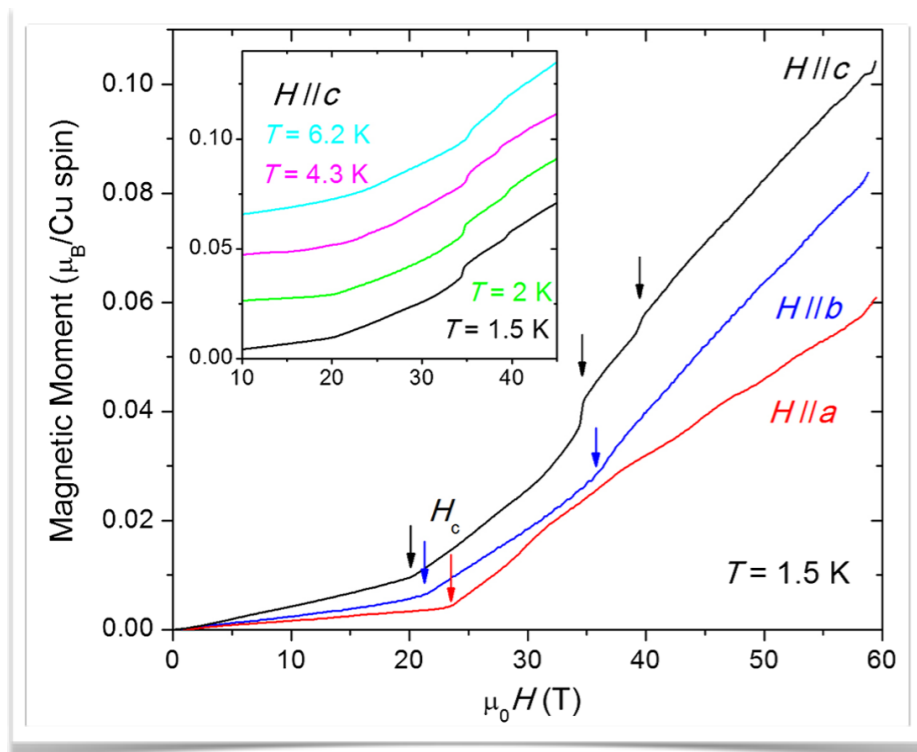
Ref.	$J_1$	$J_2$	$J_3$	$J_4$	$J_5$	$J_6$
1	1	0.67 ~ 0.79	0.41 ~ 0.69	1.0 ~ 1.2	$-2.5 \sim 2.9 \times 10^{-3}$	$-9.0 \sim 9.7 \times 10^{-3}$
2	1	0.88 ~ 0.97	-0.14 ~ 0.13	0.78 ~ 0.88	-	-

- ➡  $J_5$  &  $J_6$  are much smaller than others.
- ➡  $J_2$  (NNN in leg) may be comparable to  $J_1$ .
- ➡ Effective model corresponds to  $J_1$ - $J_2$ - $J_4$  model.

- [1] O. Mentré, *et al*, PRB 80, 180413(R) (2009).  
 [2] A. A. Tsirlin, *et al*, PRB 82, 144426 (2010).

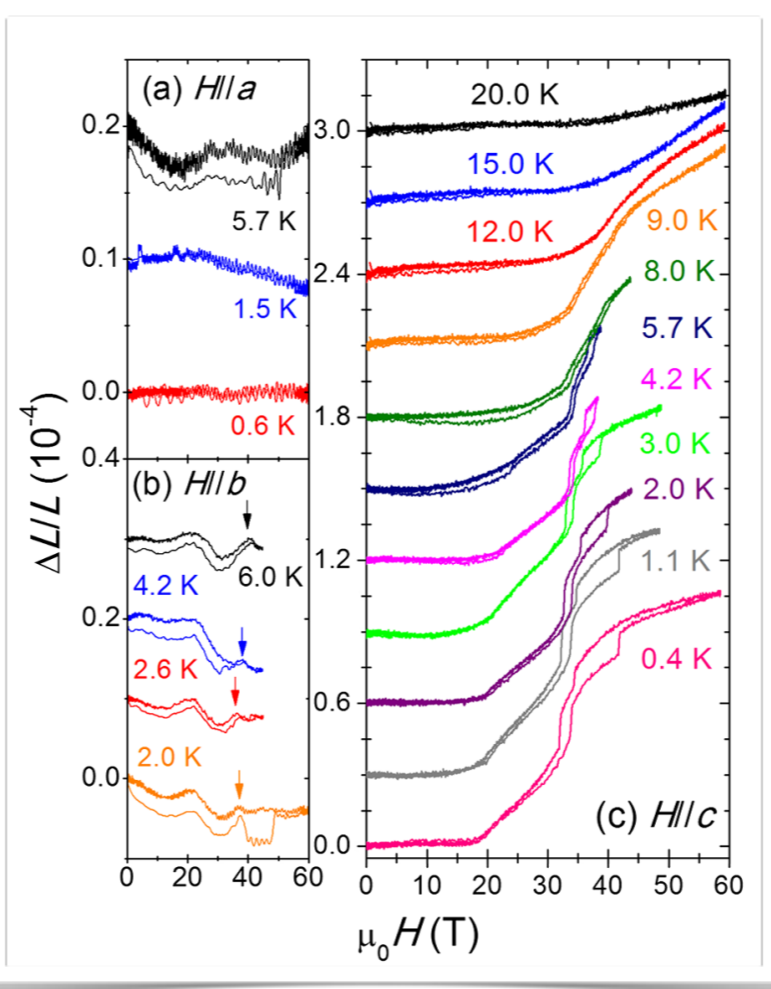
# Real compound

## M-H curve

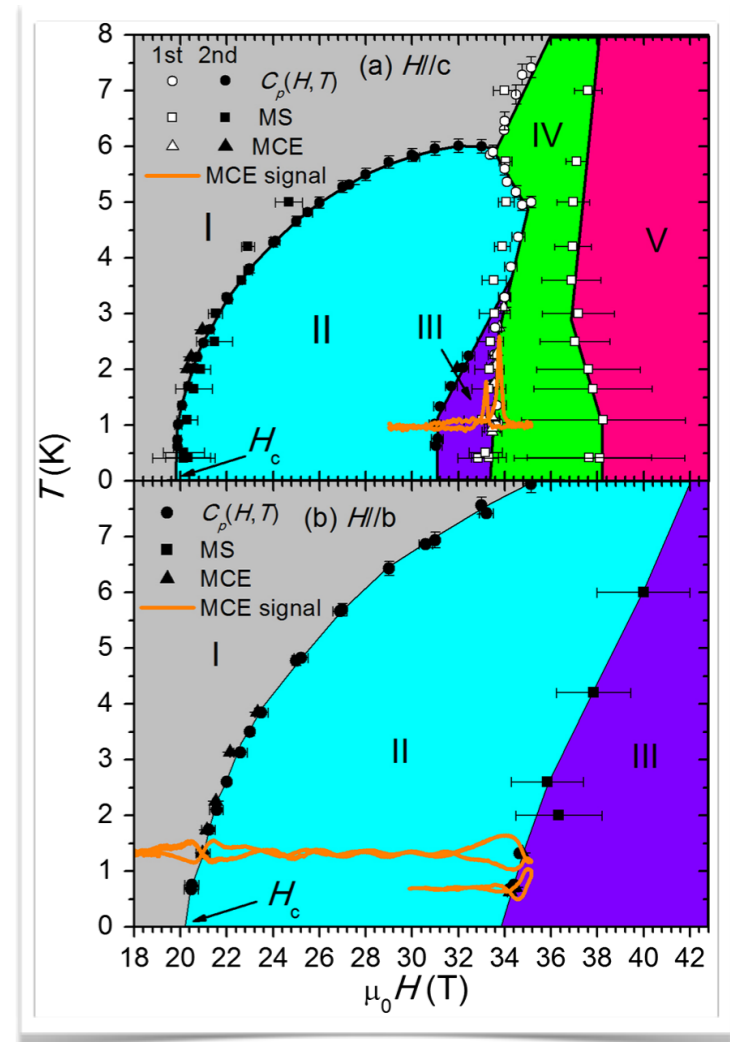


Y. Kohama, *et al*, PRL **109**, 167204 (2012).

## Magnetostriction



## Phase diagram



- ➡ M-H curve along c-axis is quite different from those along a- and b-axis.
- ➡ Phase IV & V may occur caused by spin-lattice coupling.
- ➡ Phase II & III may be spin-liquid phases.

However, the transition between two different spin-liquid phases does not appear in non-frustrated two-leg spin ladder.



# Purpose

Our purposes are

to determine the ground-state phase of  $\text{BiCu}_2\text{PO}_6$ ,  
and to clarify the phase transition induced by magnetic field.

➤ To determine the ground-state phase of  $\text{BiCu}_2\text{PO}_6$ , we use the magnetic excitation, which can be addressed by inelastic neutron scattering.

➤ The dynamical spin correlation function (DSCF):

$$\chi(\mathbf{q}, \omega) = -\frac{1}{\pi} \Im \int_0^\infty dt e^{i\omega t} \langle 0 | S^{z\dagger}(\mathbf{q}, t) S^z(\mathbf{q}, 0) | 0 \rangle$$

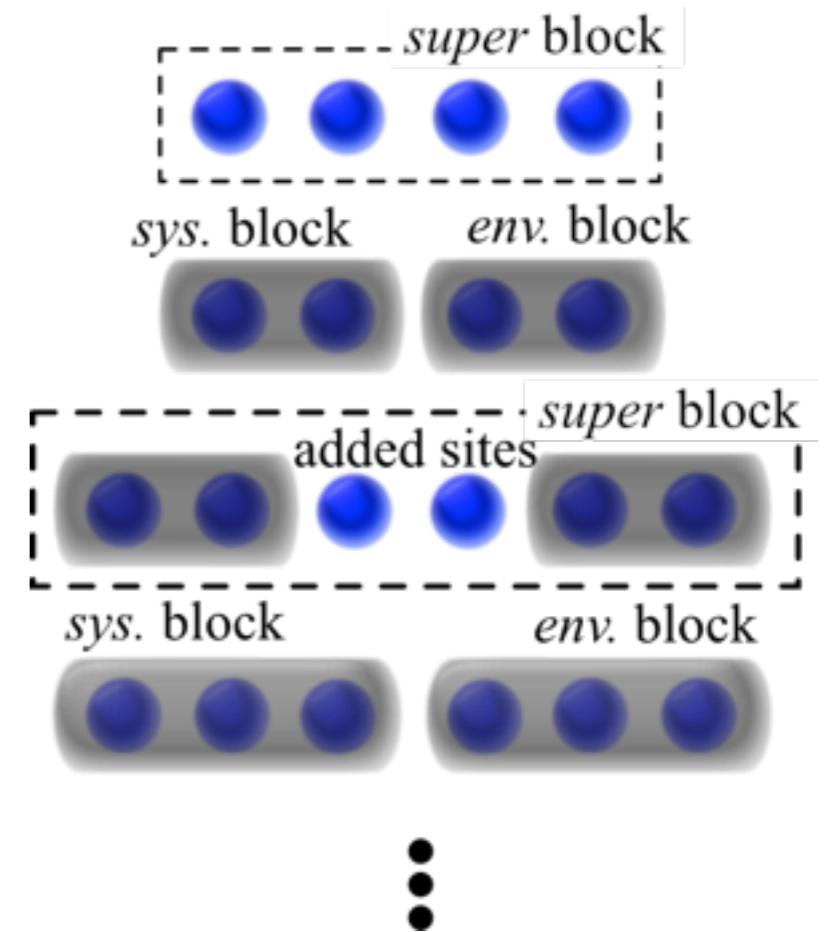
➤ To clarify the phase transition, we can use the bond-operator transform. Then, boson-like quasi-particle “triplon” is important to understand the phase transition.



# Method

## DMRG method:

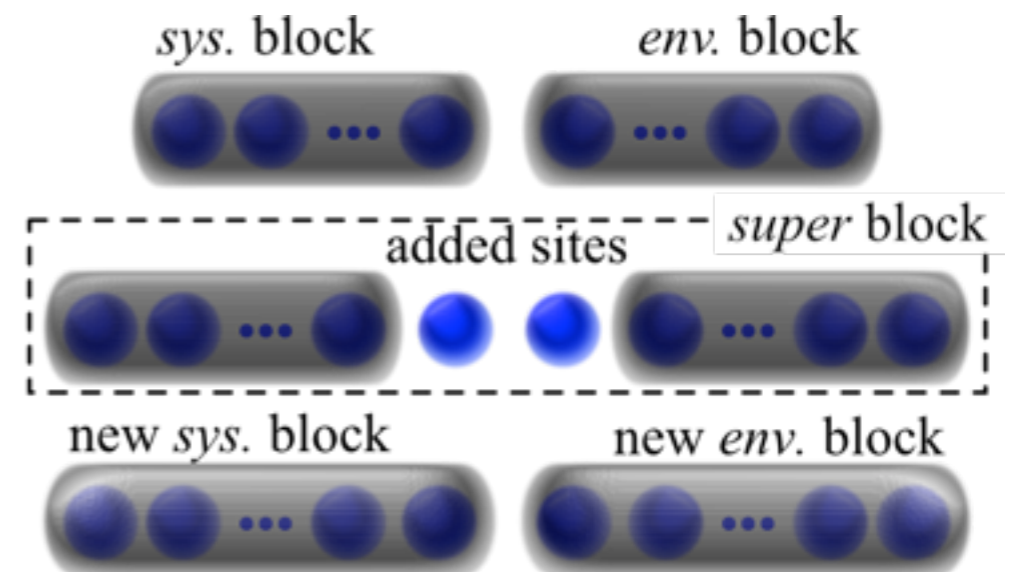
- This is a **variational method to optimize the basis** for the best description of physical quantities of interest.
- The main idea of the DMRG method is a **systematic selection of kept states** after **diagonalization of the reduced density matrix**.
- The reduced density matrix is made with proper **target states**.



# Method

Variational procedure of DMRG:

1. **Target states** are obtained for the super block.
2. **Reduced density matrix** is obtained by using the target states.
3. Diagonalization of the reduced density matrix is used to select kept states.
4. Basis of new sys. block is given by orthonormal matrix obtained by the diagonalization.



Target state (e.g. the ground state):

$$|\psi\rangle = \sum_{i,j} \psi_{ij} |i\rangle_s |j\rangle_e.$$

$|i\rangle_s$  : the basis of the **sys.** block and the **left** added site.

$|j\rangle_e$  : the basis of the **env.** block and the **right** added site.

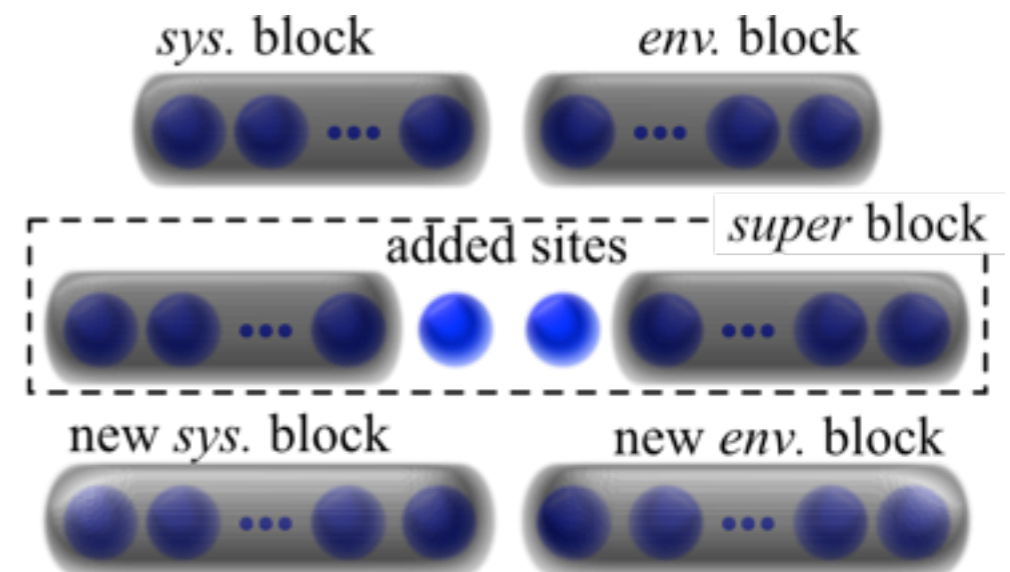
Reduced density matrix:

$$\rho_{il}^r = \sum_j \psi_{ij} \psi_{jl}^*.$$

# Method

Variational procedure of DMRG:

1. Target states are obtained for the super block.
2. Reduced density matrix is obtained by using the target states.
3. **Diagonalization of the reduced density matrix** is used to select kept states.
4. **Basis of new sys. block** is given by orthonormal matrix obtained by the diagonalization.



Diagonalization of RDM:

$$\rho_{il}^r = \sum_k U_{ik}^* \Lambda_{kk}^2 U_{kl}.$$

$\Lambda_{kk}$  : diagonal matrix.

$U_{kl}$  : unitary matrix.

Basis of new sys. block:

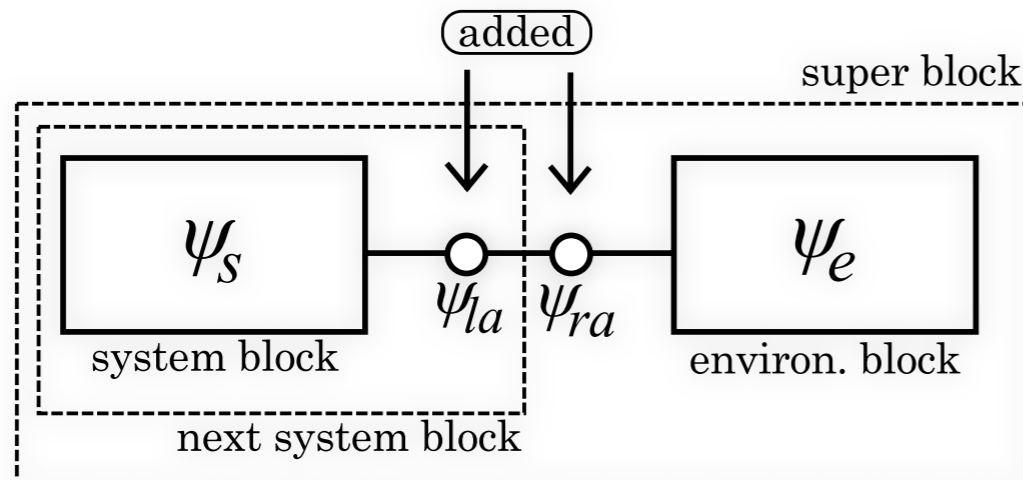
$$|u^\alpha\rangle_s = \sum_i U_{i\alpha}^* |i\rangle_s.$$

$\alpha = 1, 2, \dots, M.$

$M$  : truncation number of DMRG.

# Method

- ◆ Density-matrix renormalization-group method



- ◆ Dynamical spin correlation function

$$\begin{aligned}\chi(\mathbf{q}, \omega) &= -\frac{1}{\pi} \Im \int_0^\infty dt e^{i(\omega+i\gamma)t} \langle 0 | \mathbf{S}^\dagger(\mathbf{q}, t) \cdot \mathbf{S}(\mathbf{q}, 0) | 0 \rangle \\ &= -\frac{1}{\pi} \Im \langle 0 | \mathbf{S}^\dagger(\mathbf{q}) \frac{1}{\omega - \mathcal{H} + E_0 + i\gamma} \mathbf{S}(\mathbf{q}) | 0 \rangle.\end{aligned}$$

- ◆ Target states

$$|0\rangle, \mathbf{S}(\mathbf{q})|0\rangle, \text{ and } \frac{1}{\omega - \mathcal{H} + E_0 + i\gamma} \mathbf{S}(\mathbf{q})|0\rangle.$$

- ➡ We use the DMRG method to obtain the DSCF numerically.
- ➡ We calculate the DSCF in 32\*2 sites ladder.

# Numerical Results

## DSCF for three points:

a, b) Incomm. CD phase (★)

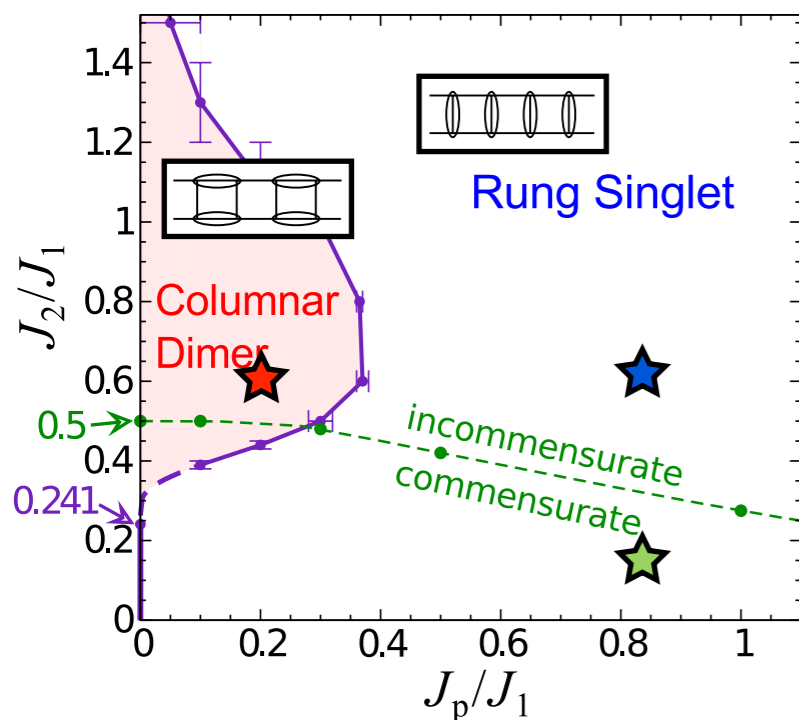
$$J_2/J_1=0.6, J_p/J_1=0.2$$

c, d) Comm. RS phase (★)

$$J_2/J_1=0.1, J_p/J_1=1.0$$

e, f) Incomm. RS phase (★)

$$J_2/J_1=0.6, J_p/J_1=1.0$$



A. Lavarélo, *et al*, PRB 84, 144407 (2011).

# Numerical Results

## DSCF for three points:

a, b) Incomm. CD phase (★)

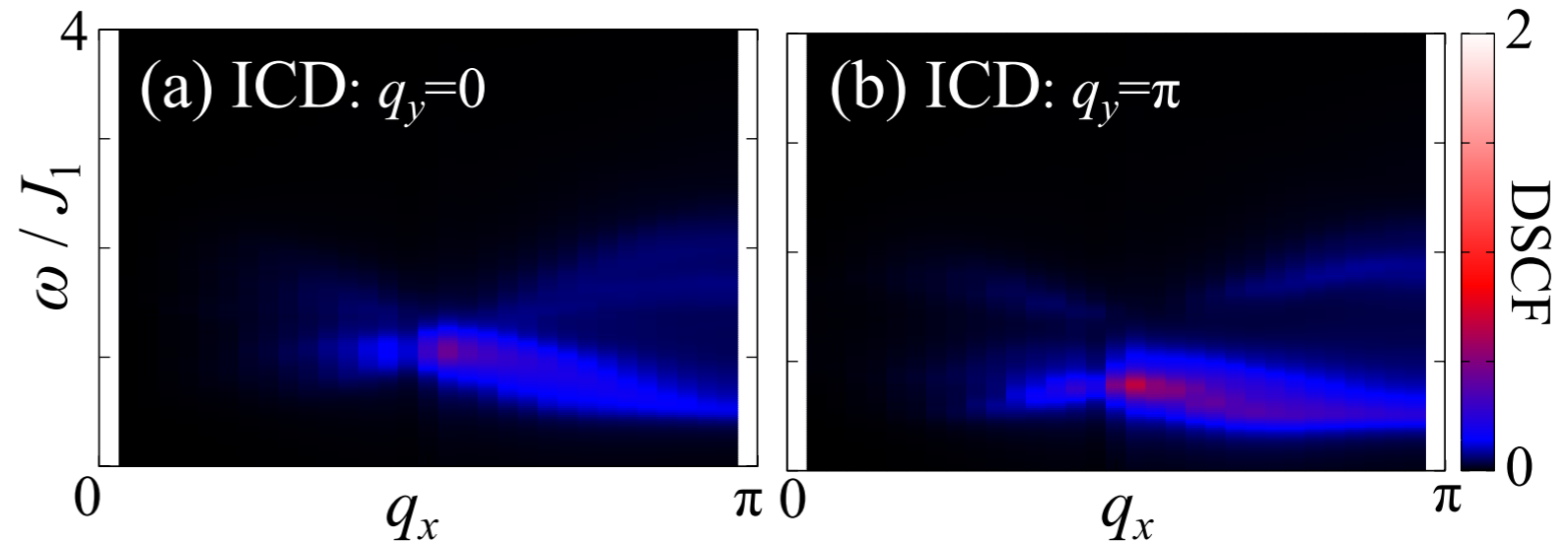
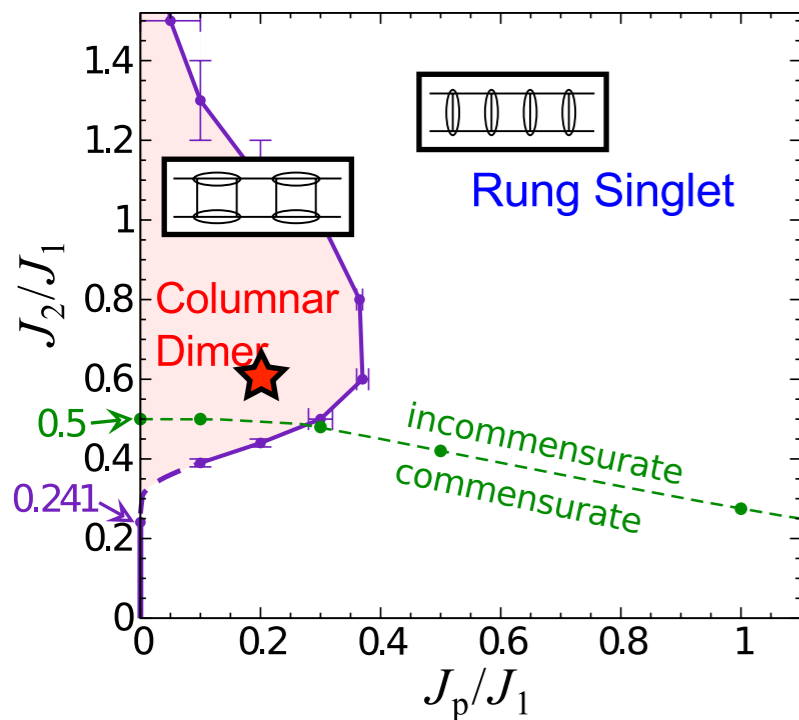
$$J_2/J_1=0.6, J_p/J_1=0.2$$

c, d) Comm. RS phase (★)

$$J_2/J_1=0.1, J_p/J_1=1.0$$

e, f) Incomm. RS phase (★)

$$J_2/J_1=0.6, J_p/J_1=1.0$$



# Numerical Results

## DSCF for three points:

a, b) Incomm. CD phase (★)

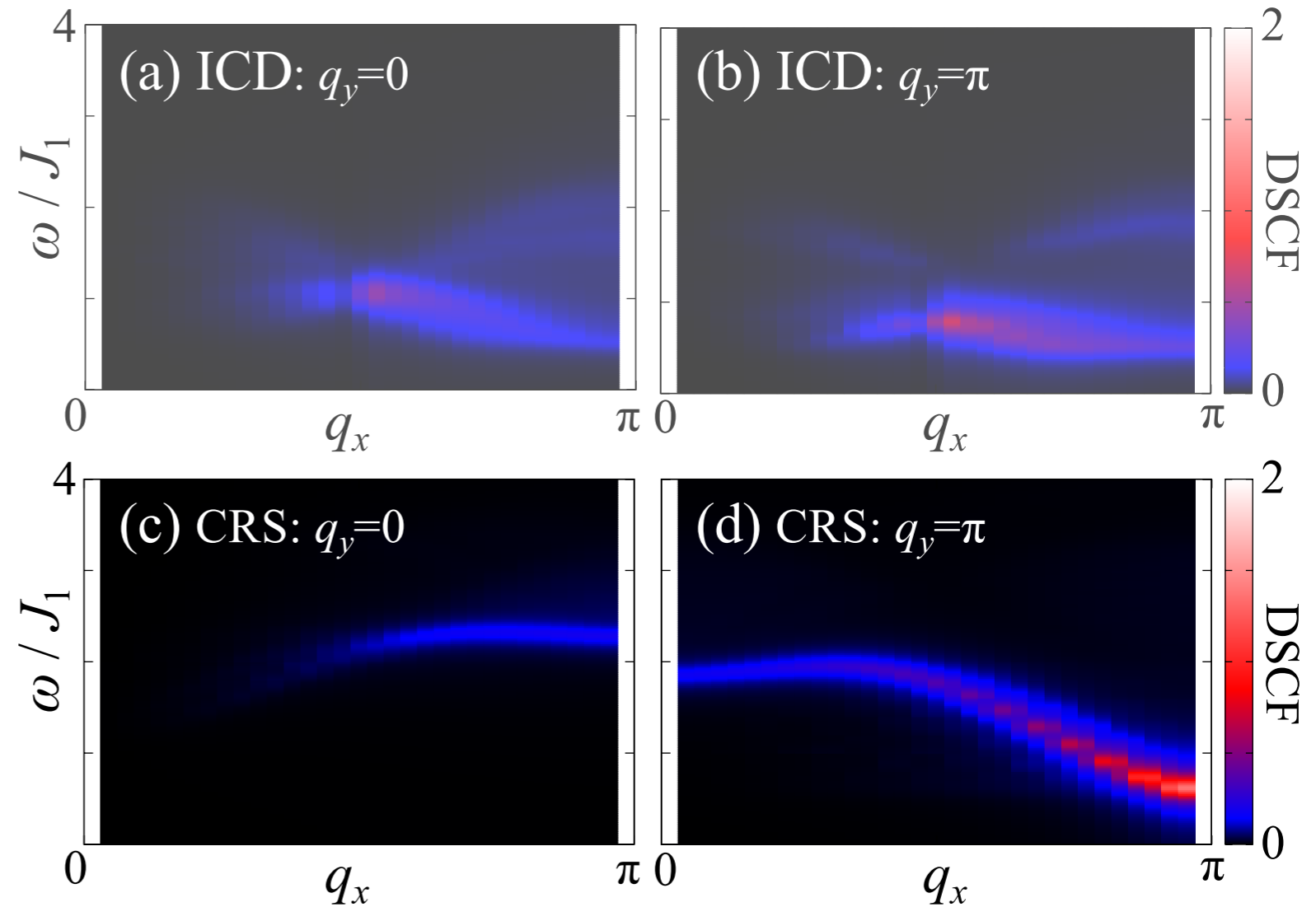
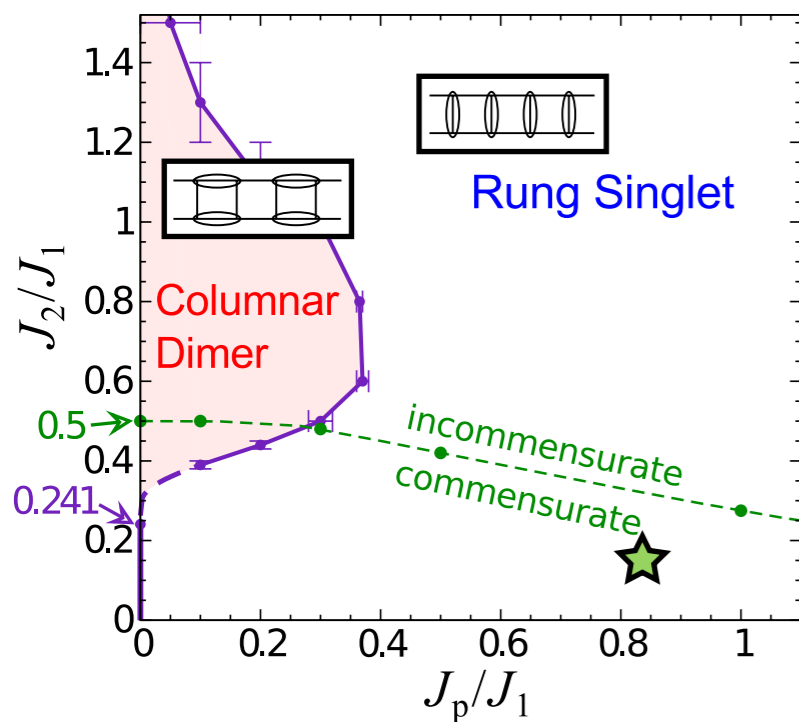
$$J_2/J_1=0.6, J_p/J_1=0.2$$

c, d) Comm. RS phase (★)

$$J_2/J_1=0.1, J_p/J_1=1.0$$

e, f) Incomm. RS phase (★)

$$J_2/J_1=0.6, J_p/J_1=1.0$$



# Numerical Results

## DSCF for three points:

a, b) Incomm. CD phase (★)

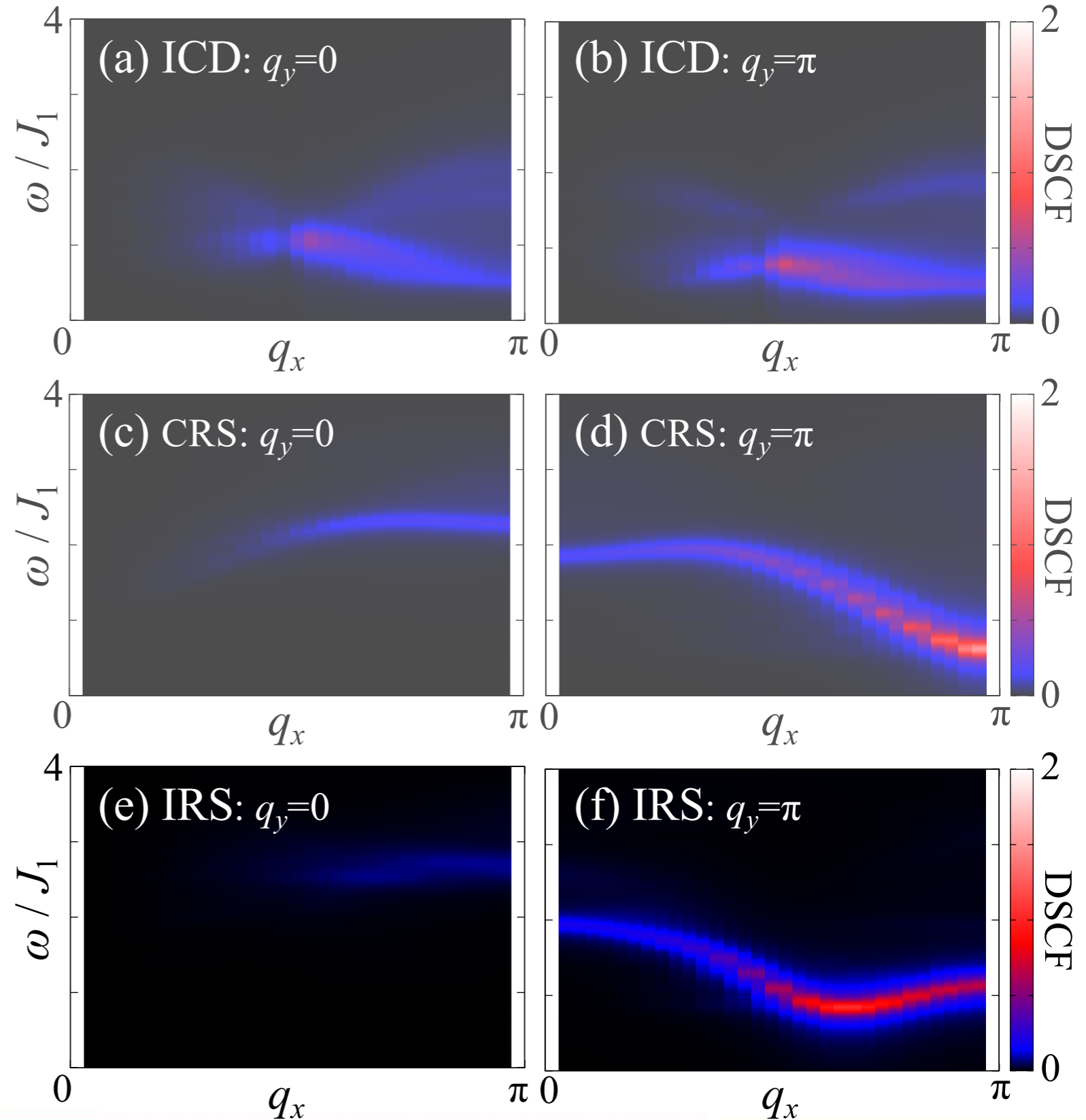
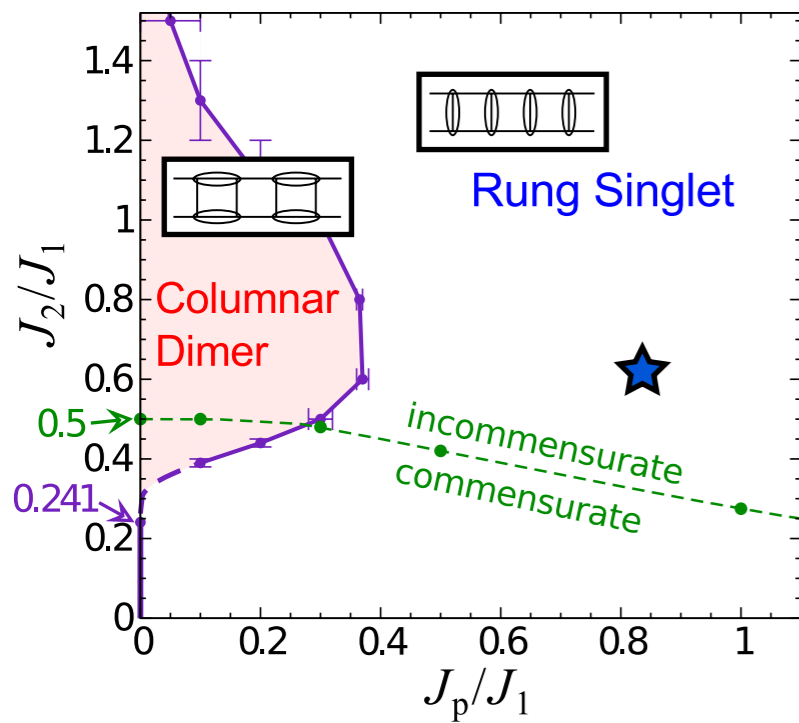
$$J_2/J_1=0.6, J_p/J_1=0.2$$

c, d) Comm. RS phase (★)

$$J_2/J_1=0.1, J_p/J_1=1.0$$

e, f) Incomm. RS phase (★)

$$J_2/J_1=0.6, J_p/J_1=1.0$$





# Numerical Results

## DSCF for three points:

a, b) Incomm. CD phase (★)

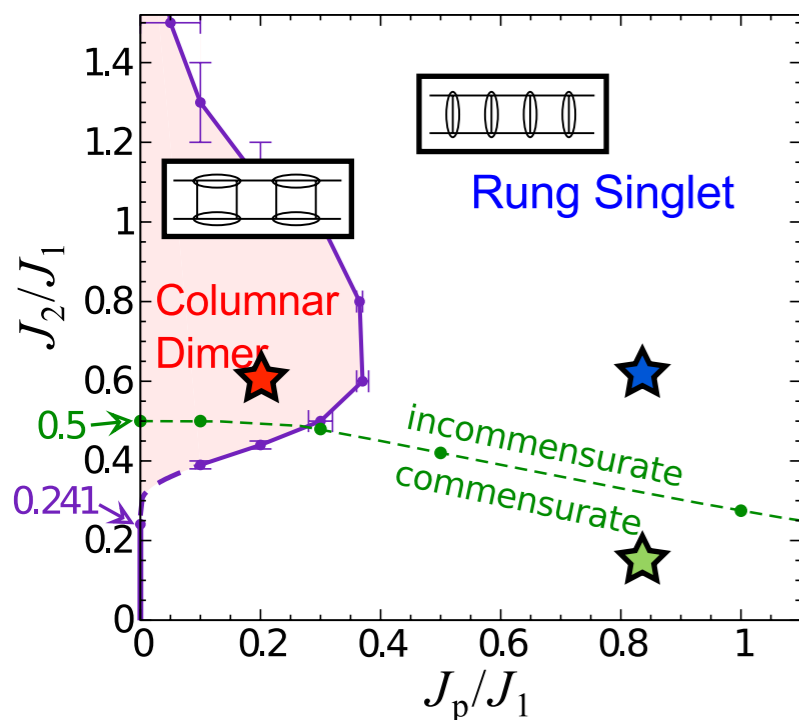
$$J_2/J_1=0.6, J_p/J_1=0.2$$

c, d) Comm. RS phase (★)

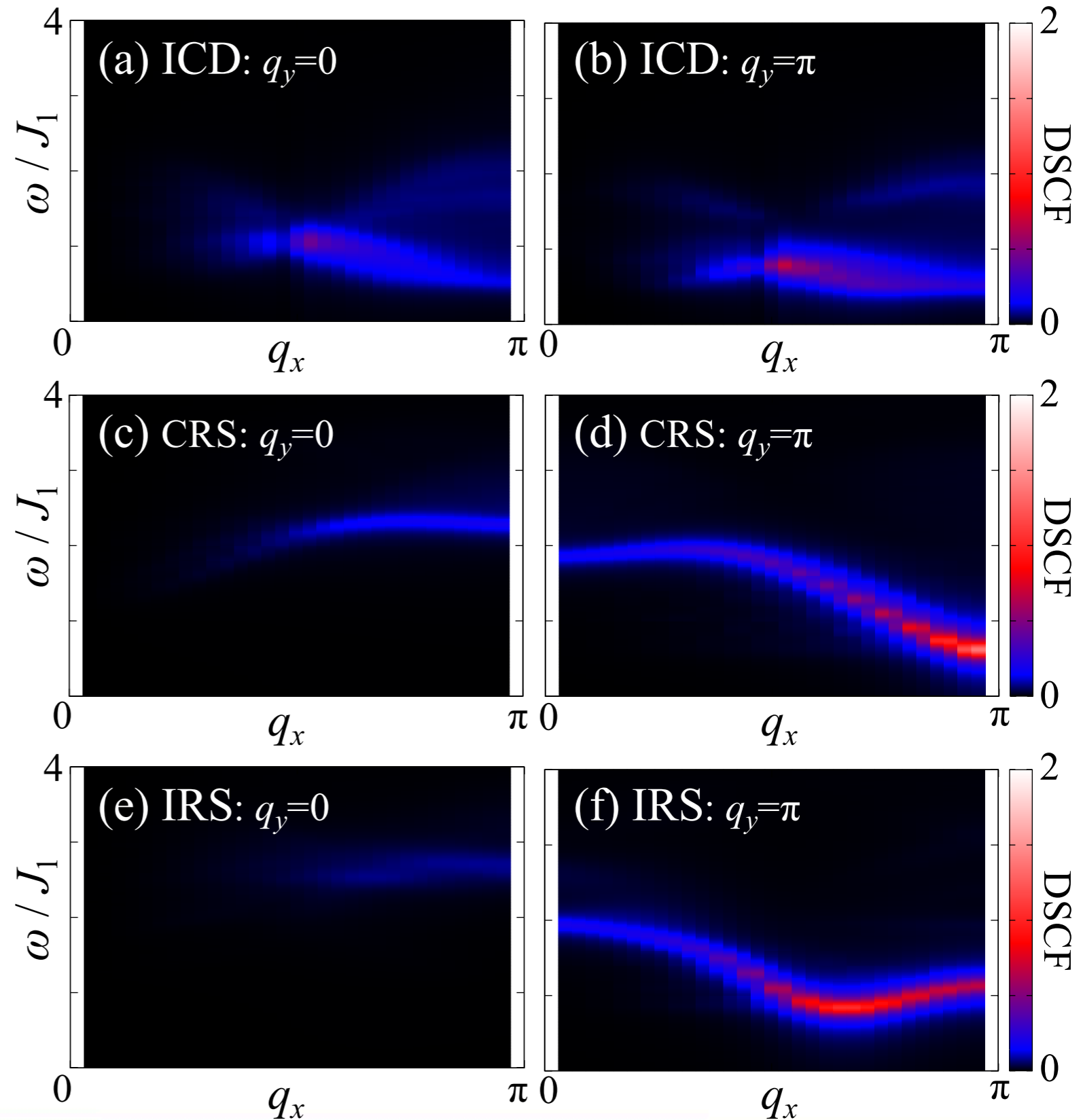
$$J_2/J_1=0.1, J_p/J_1=1.0$$

e, f) Incomm. RS phase (★)

$$J_2/J_1=0.6, J_p/J_1=1.0$$

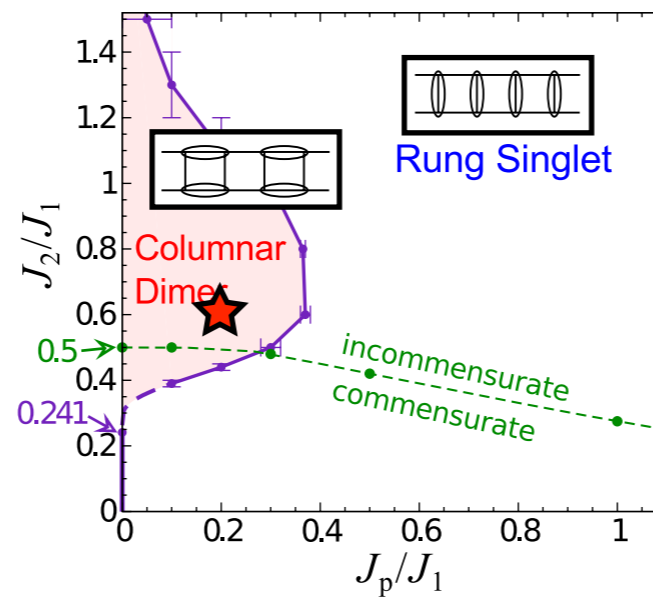
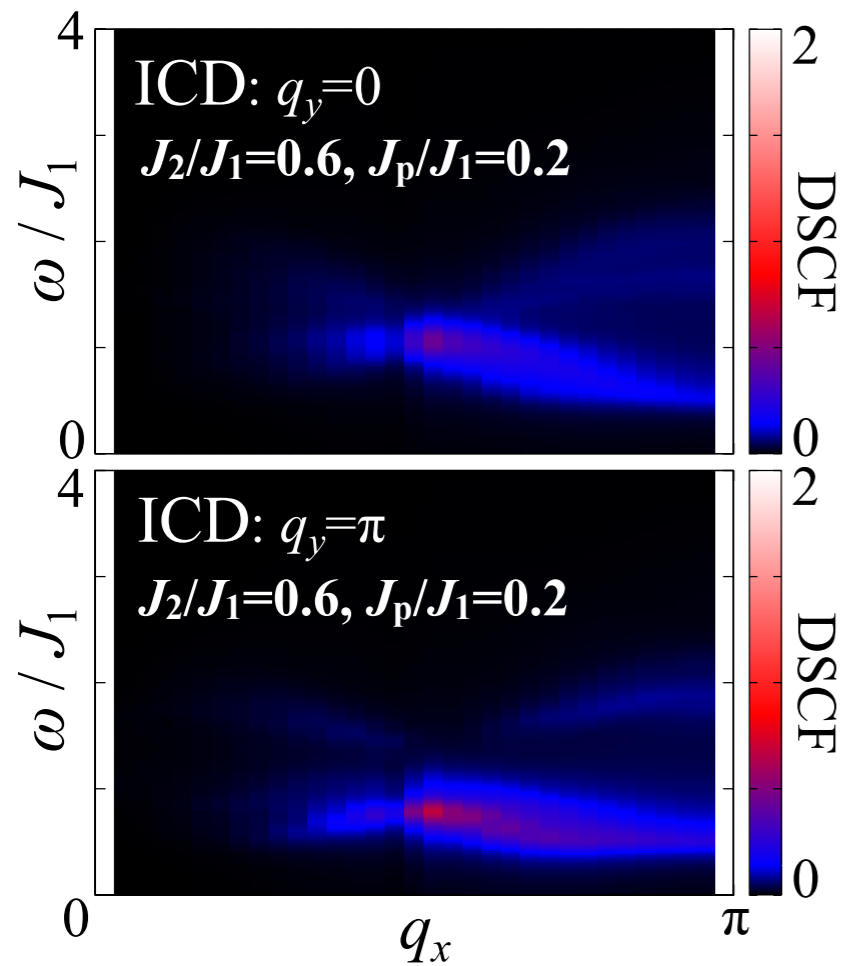


☞ We can distinguish CD and RS phases by **comparing the spectral weight** in  $q_y=0$  plane with that of  $q_y=\pi$ .



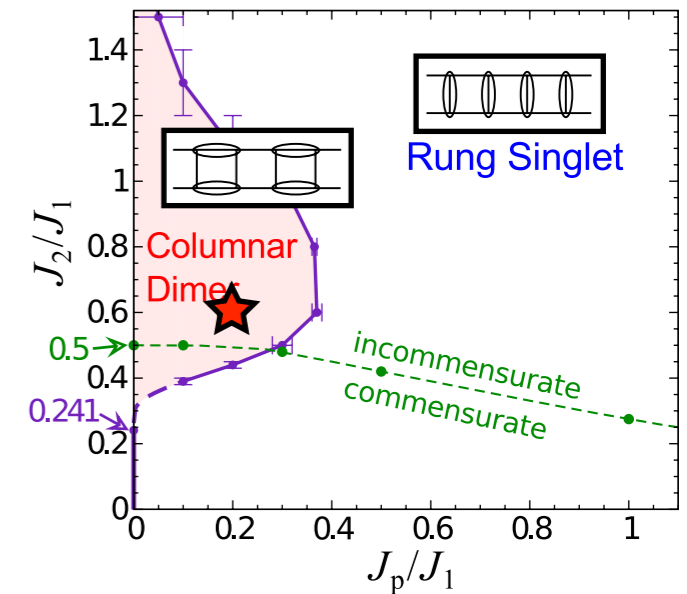
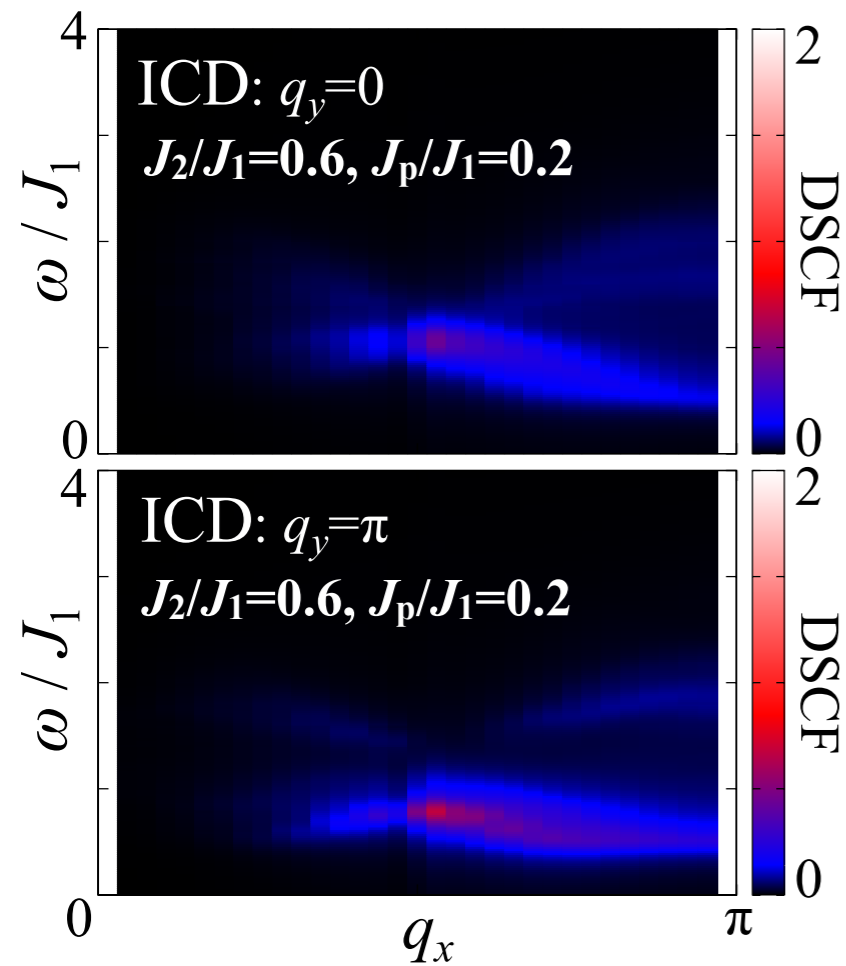
# Result: Columnar-Dimer phase

DSCF in Incomm. CD phase:



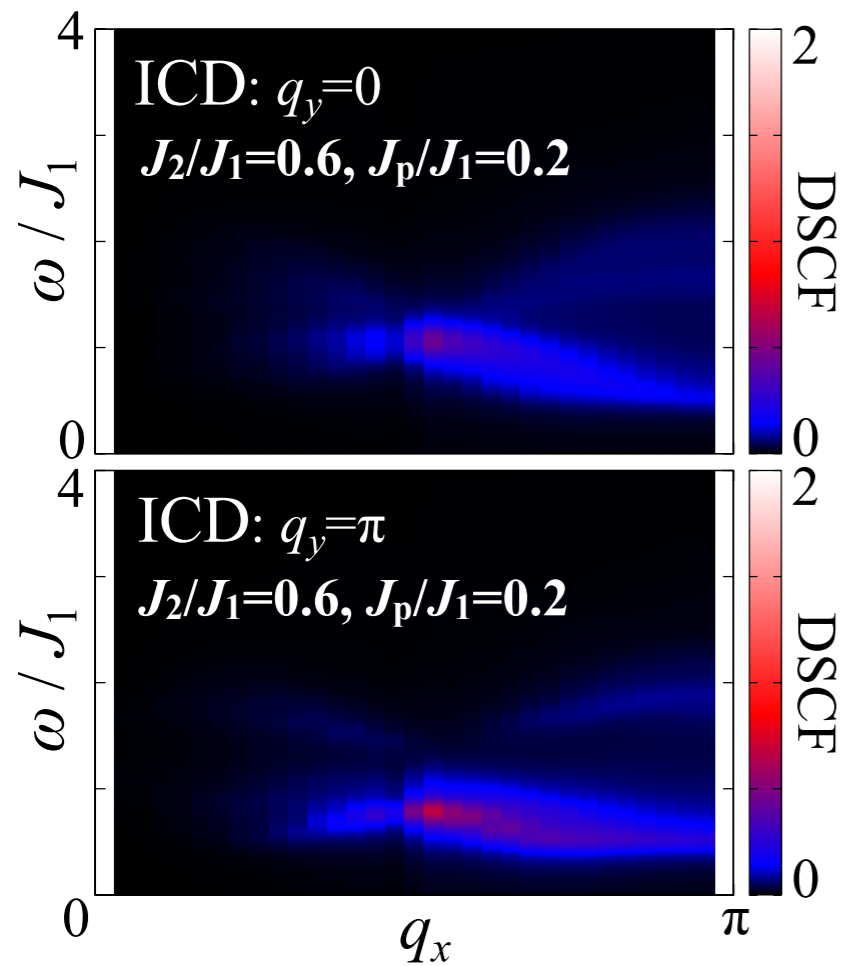
# Result: Columnar-Dimer phase

DSCF in Incomm. CD phase:

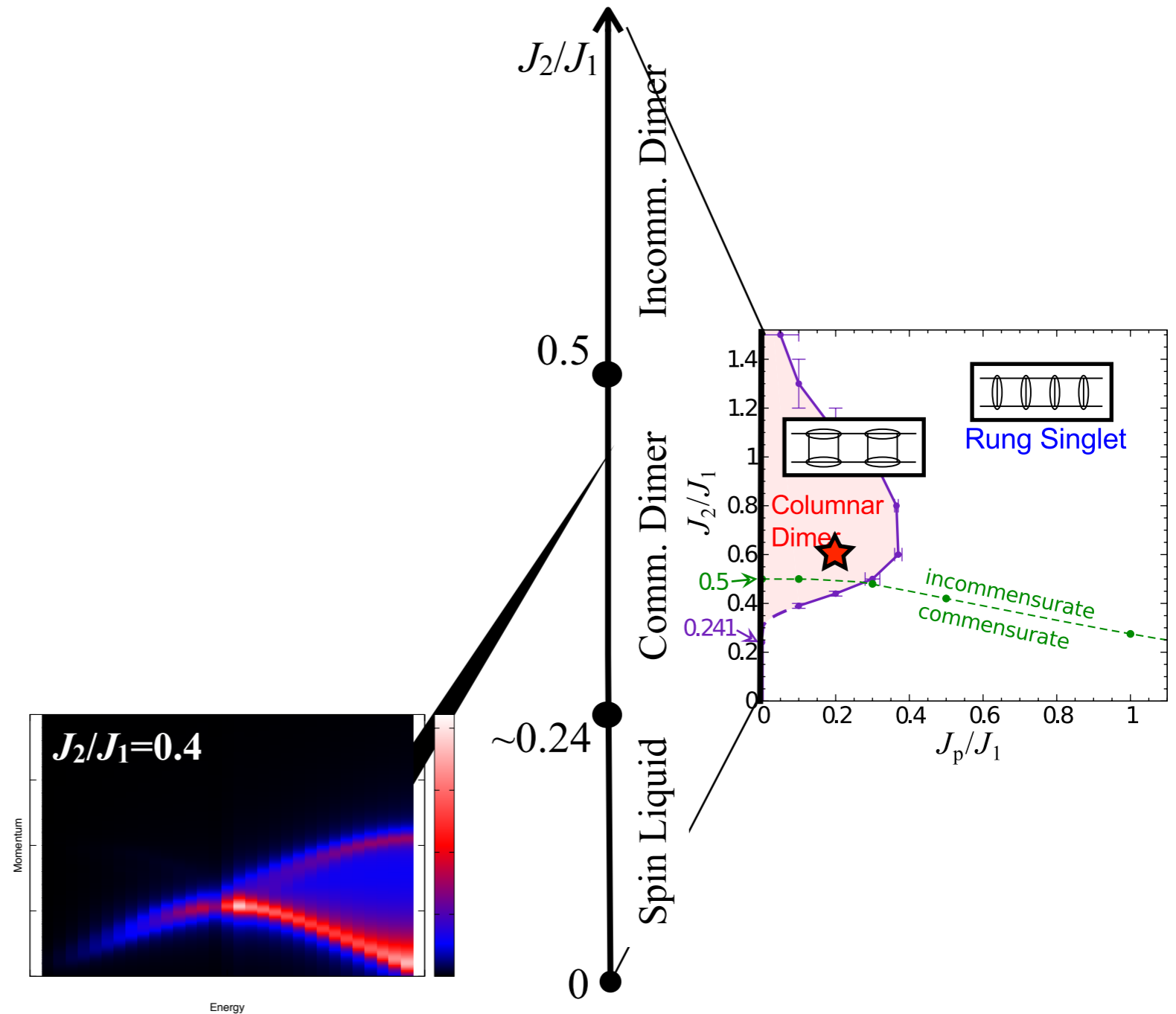


# Result: Columnar-Dimer phase

DSCF in Incomm. CD phase:

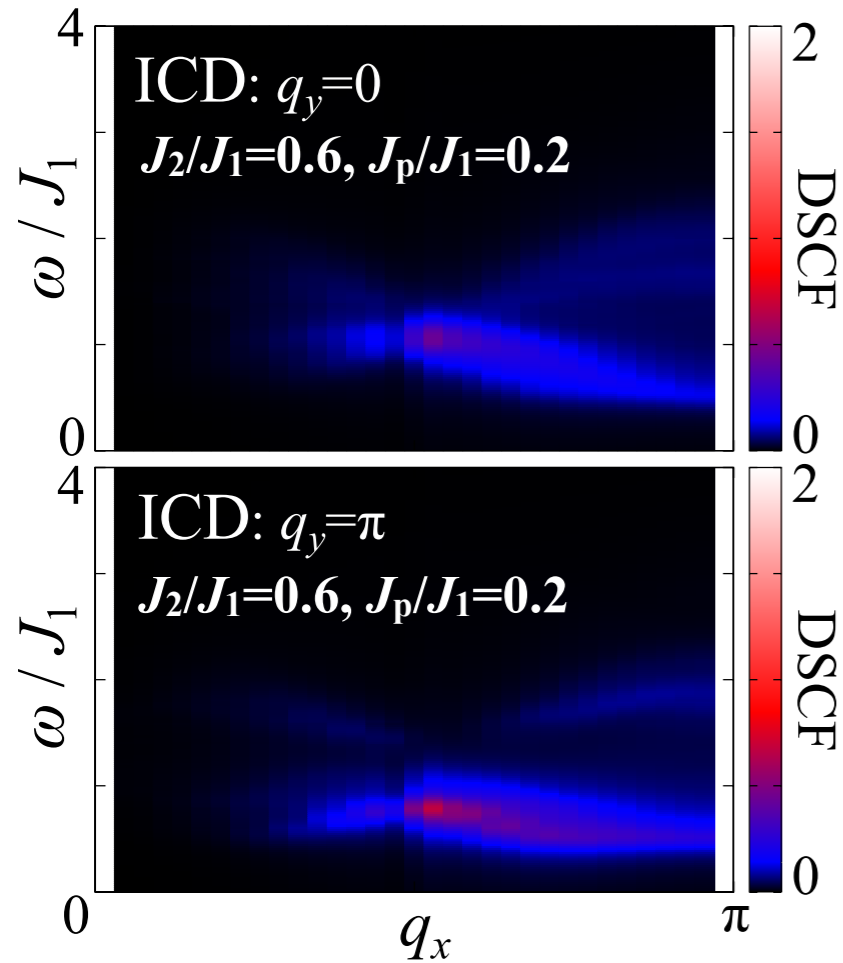


DSCF for Frustrated spin chain ( $J_p=0$ )

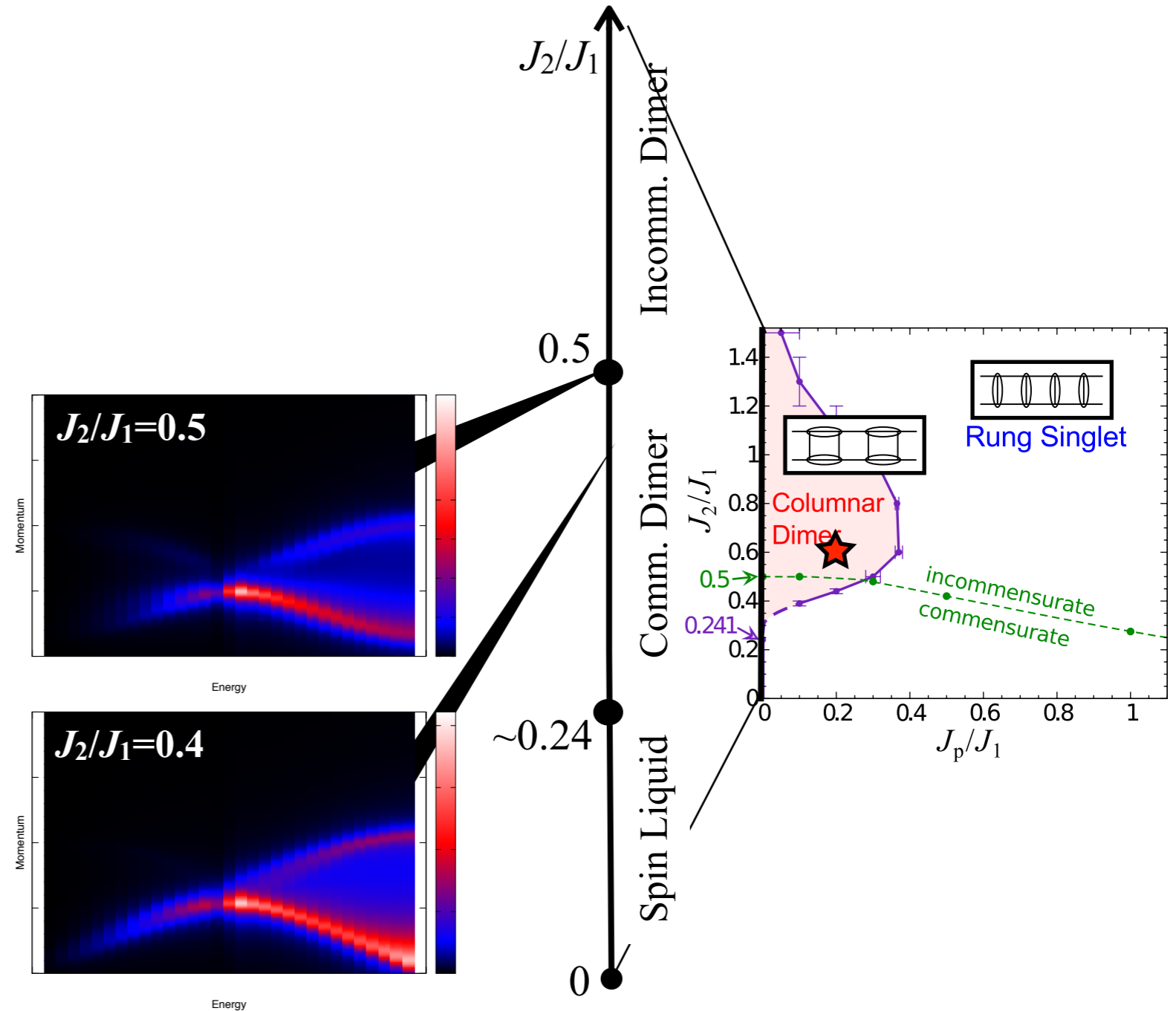


# Result: Columnar-Dimer phase

DSCF in Incomm. CD phase:

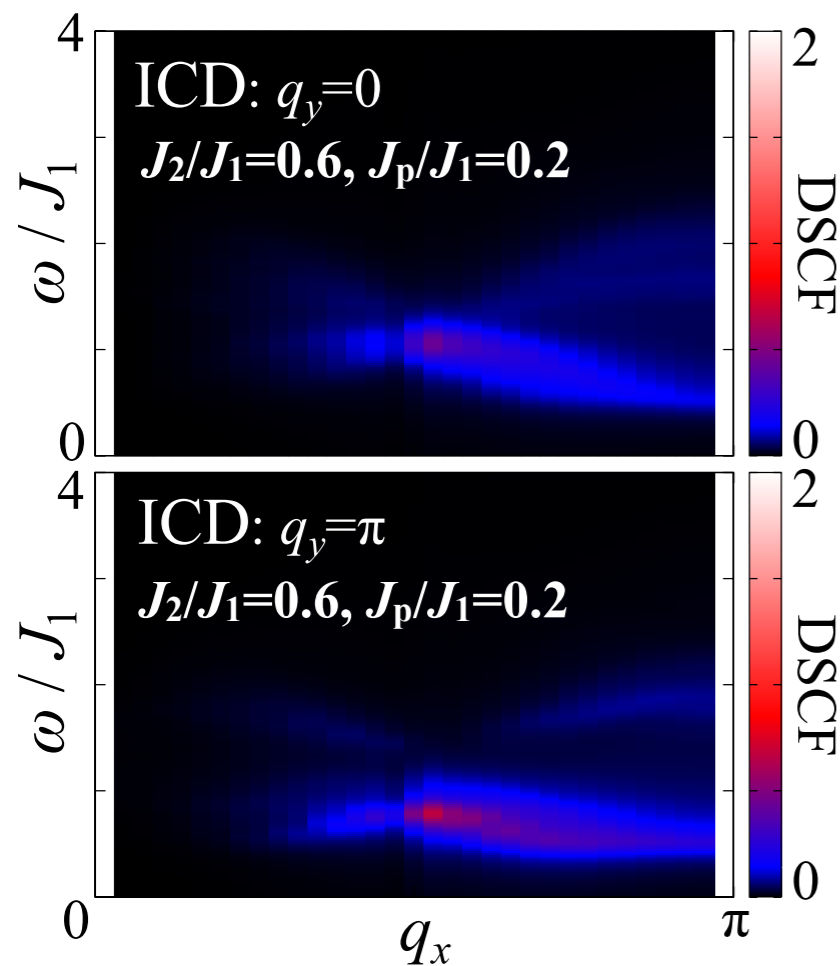


DSCF for Frustrated spin chain ( $J_p=0$ )

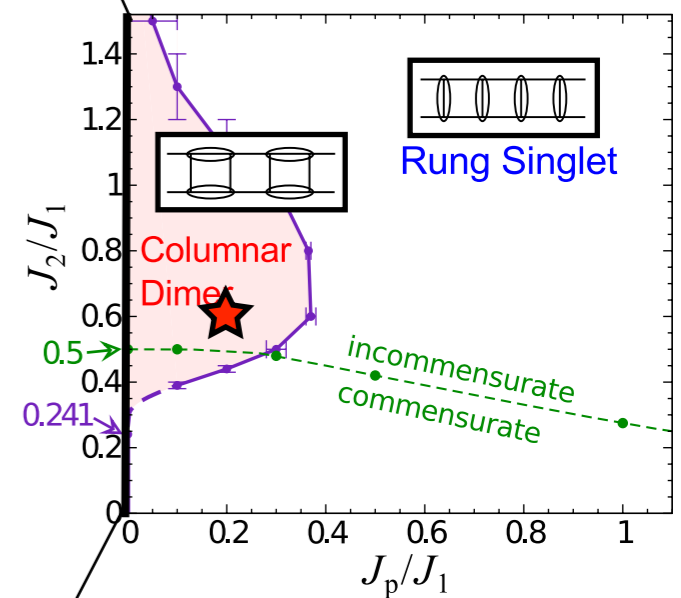
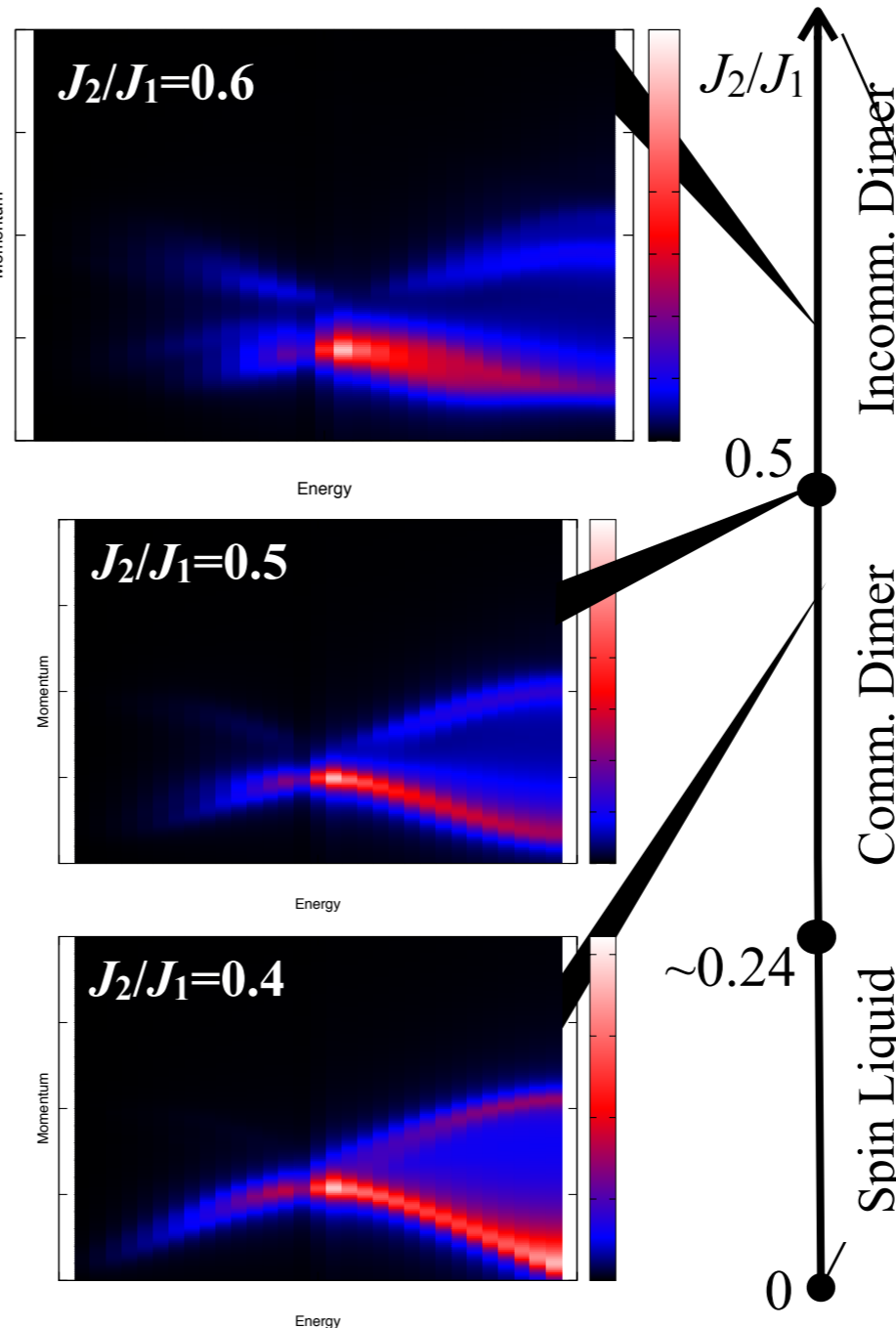


# Result: Columnar-Dimer phase

DSCF in Incomm. CD phase:



DSCF for Frustrated spin chain ( $J_p=0$ )

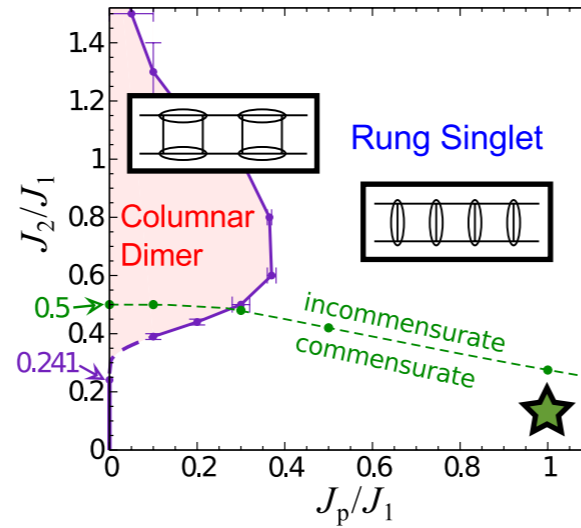
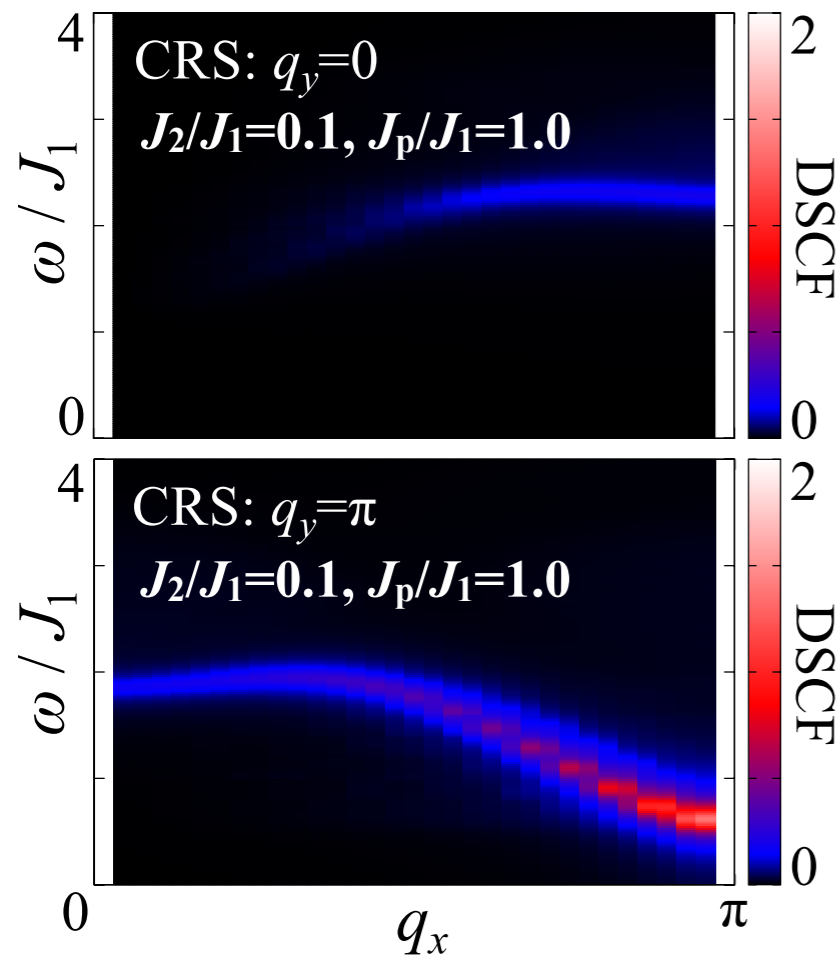


➡ The DSCF in incomm. CD phase is quite similar to that for the spin chain with frustration.

➡ Elementary excitations are **spinons**, which are not bounded on rung bond.

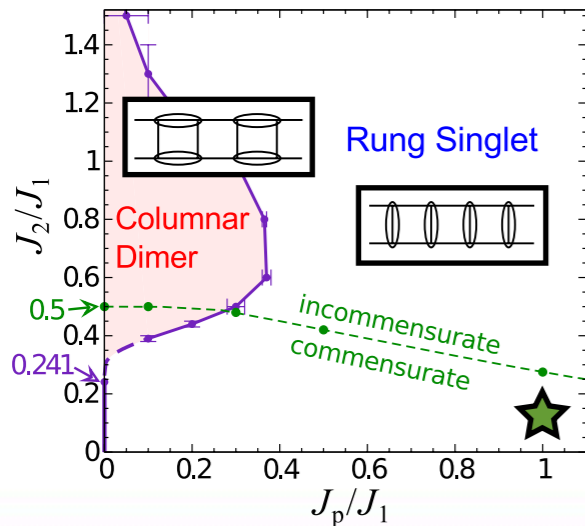
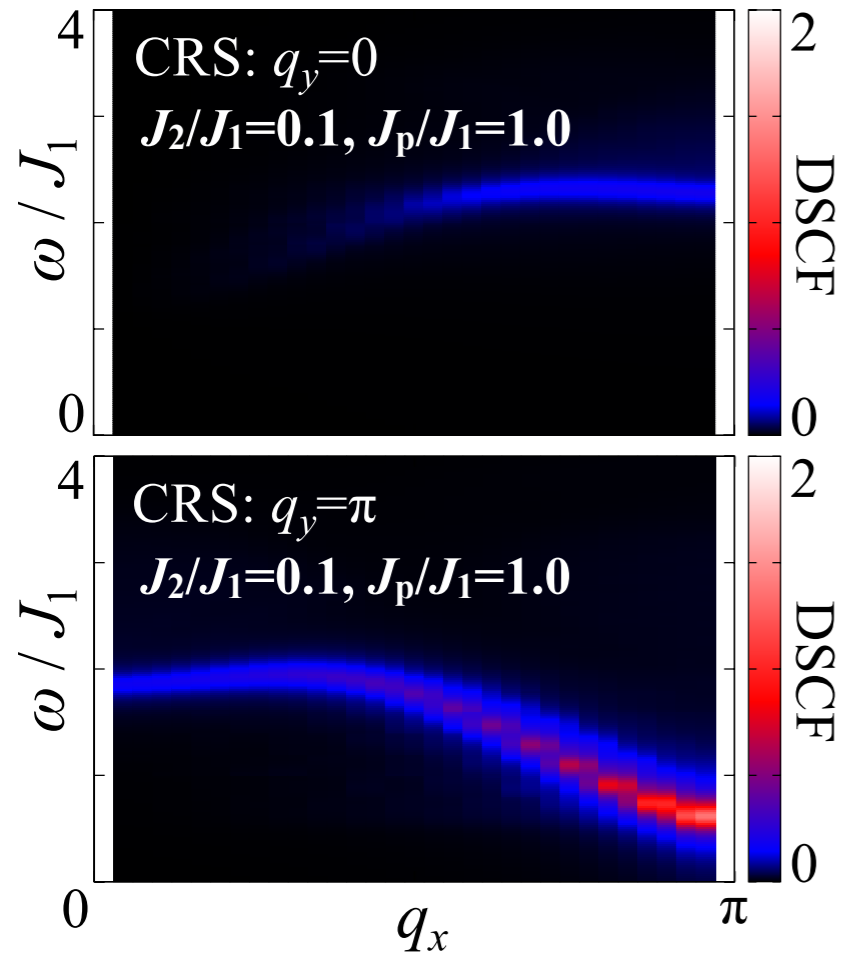
# Result: Rung-Singlet phase

DSCF in Comm. RS phase:



# Result: Rung-Singlet phase

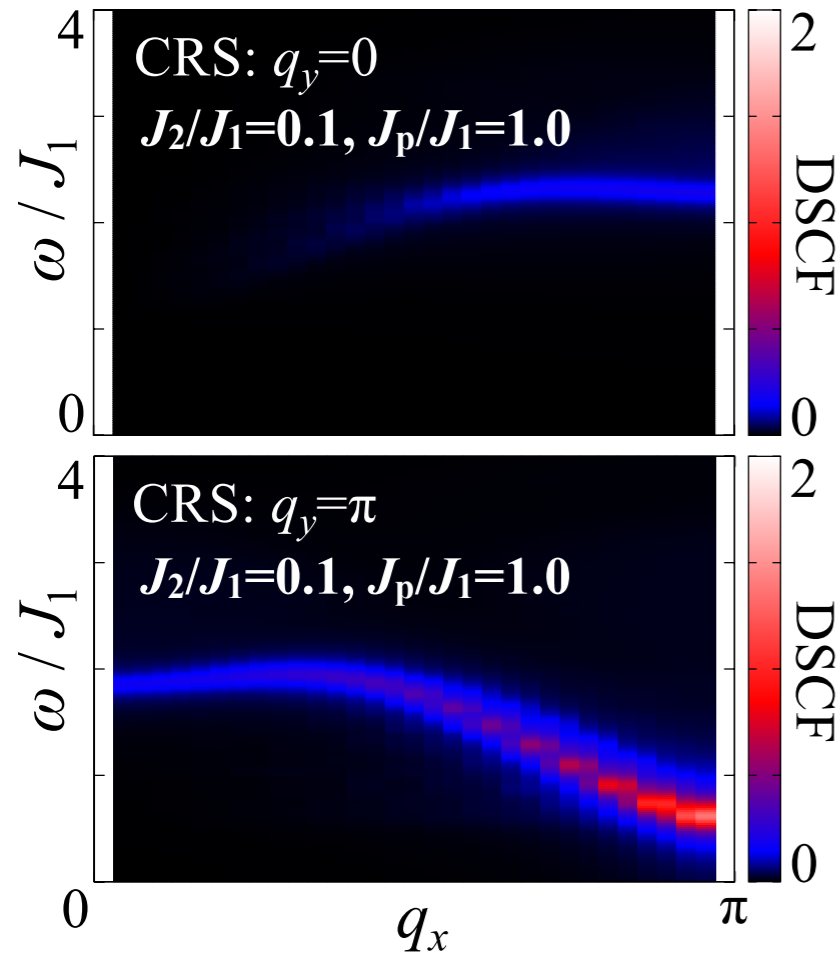
DSCF in Comm. RS phase:



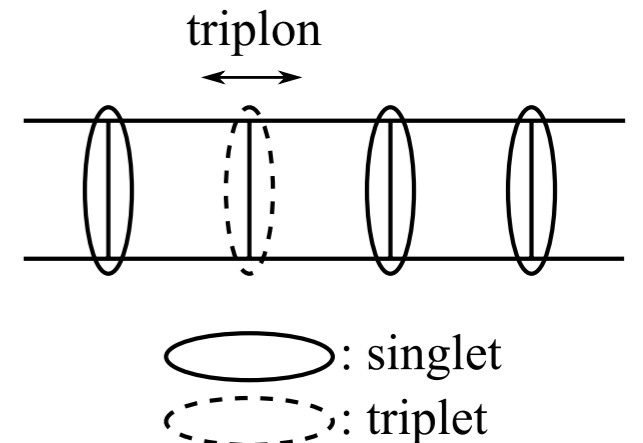
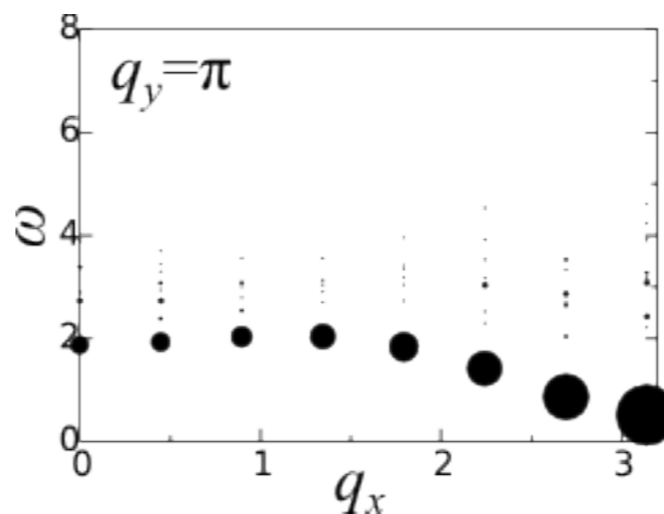


# Result: Rung-Singlet phase

DSCF in Comm. RS phase:

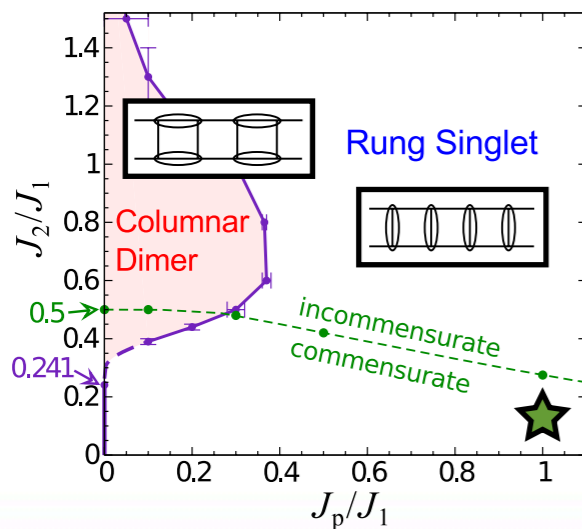


DSCF for Non-frustrated spin ladder



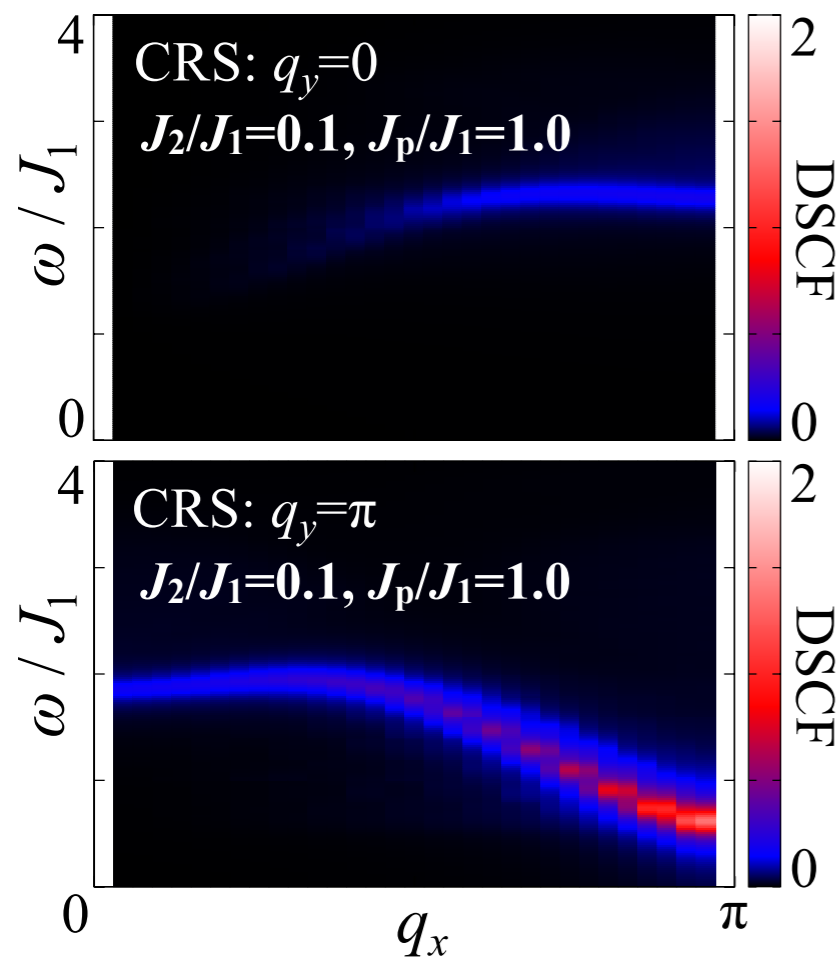
N. Haga and S. Suga, PRB **66**,132415 (2002).

➡ In comm. RS phase, anti-bonding mode ( $q_y=\pi$ ) can be understood as **triplon** mode for non-frustrated spin ladder.

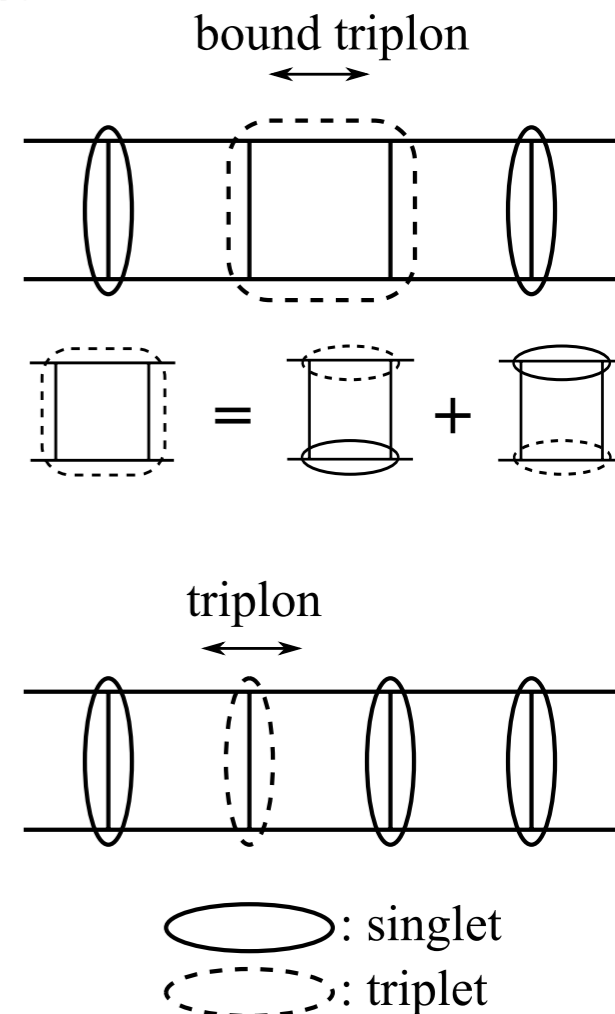
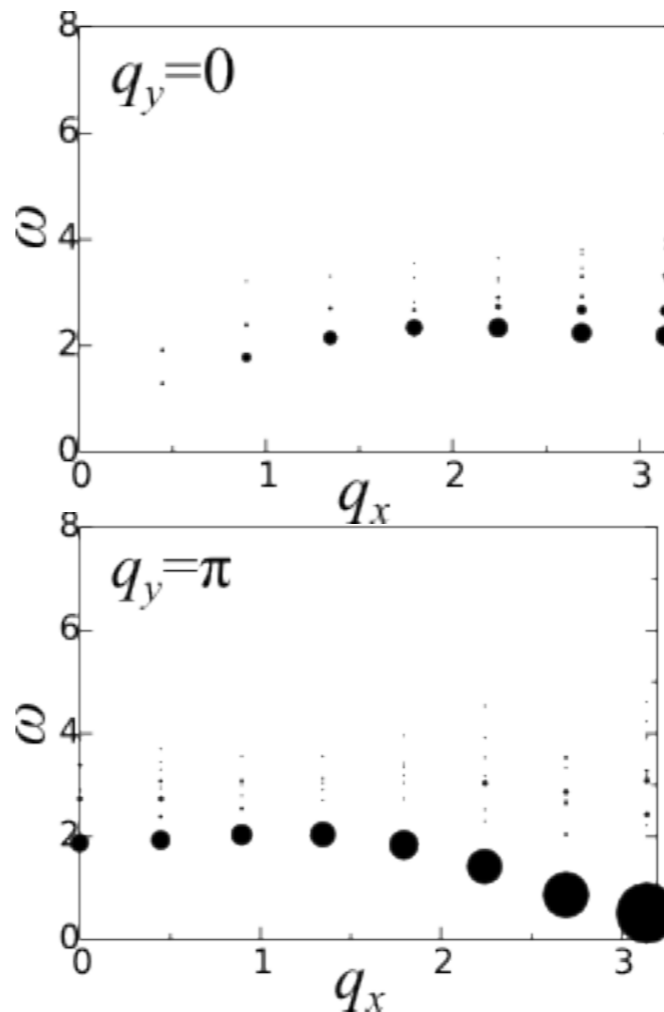


# Result: Rung-Singlet phase

DSCF in Comm. RS phase:

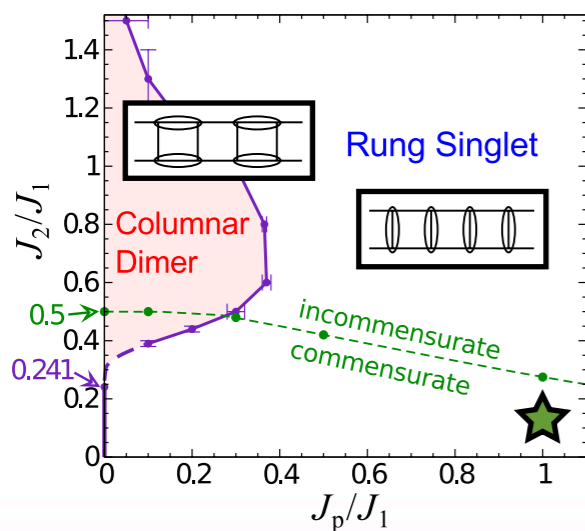


DSCF for Non-frustrated spin ladder



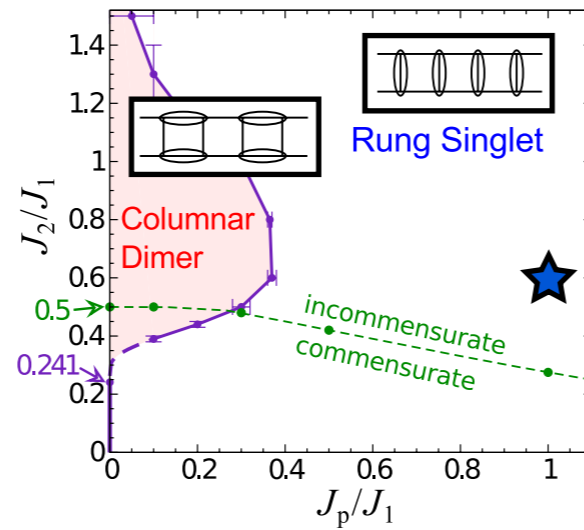
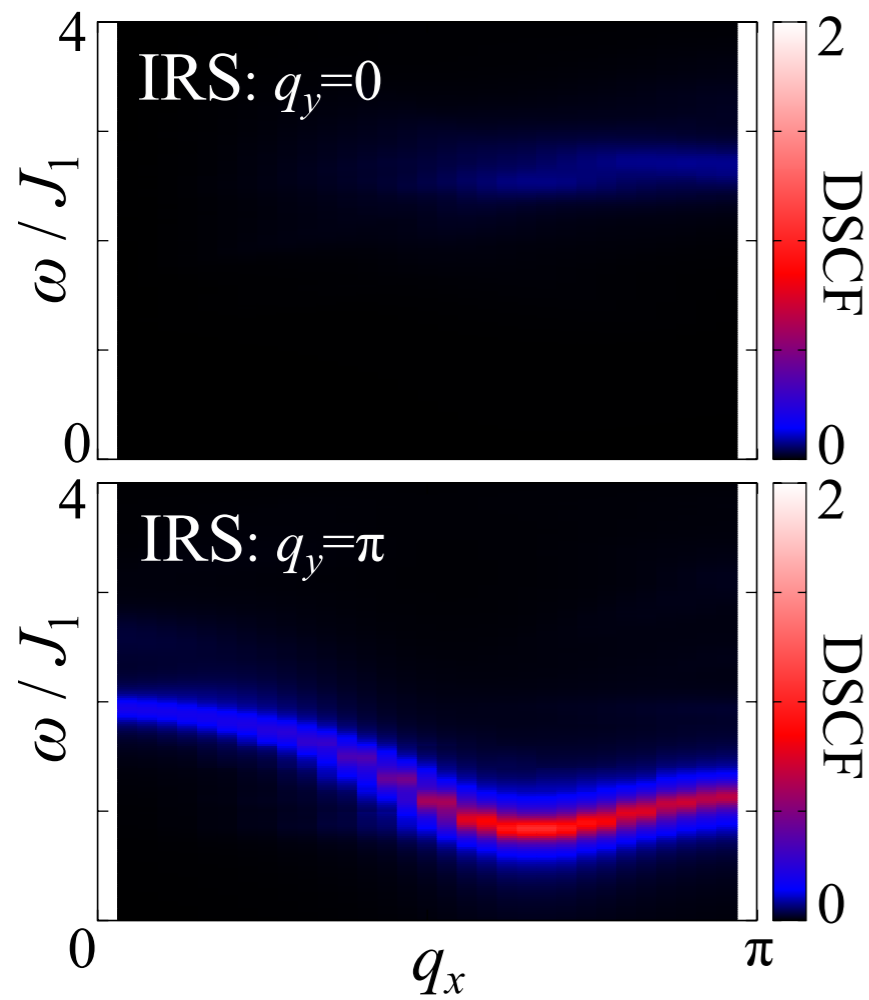
N. Haga and S. Suga, PRB **66**,132415 (2002).

- ➡ In comm. RS phase, anti-bonding mode ( $q_y=\pi$ ) can be understood as **triplon** mode for non-frustrated spin ladder.
- ➡ Bonding mode ( $q_y=0$ ) can be understood as the mode of **bound triplon**.



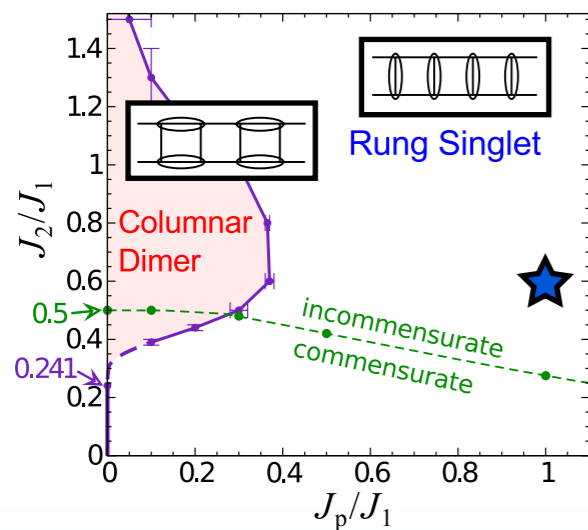
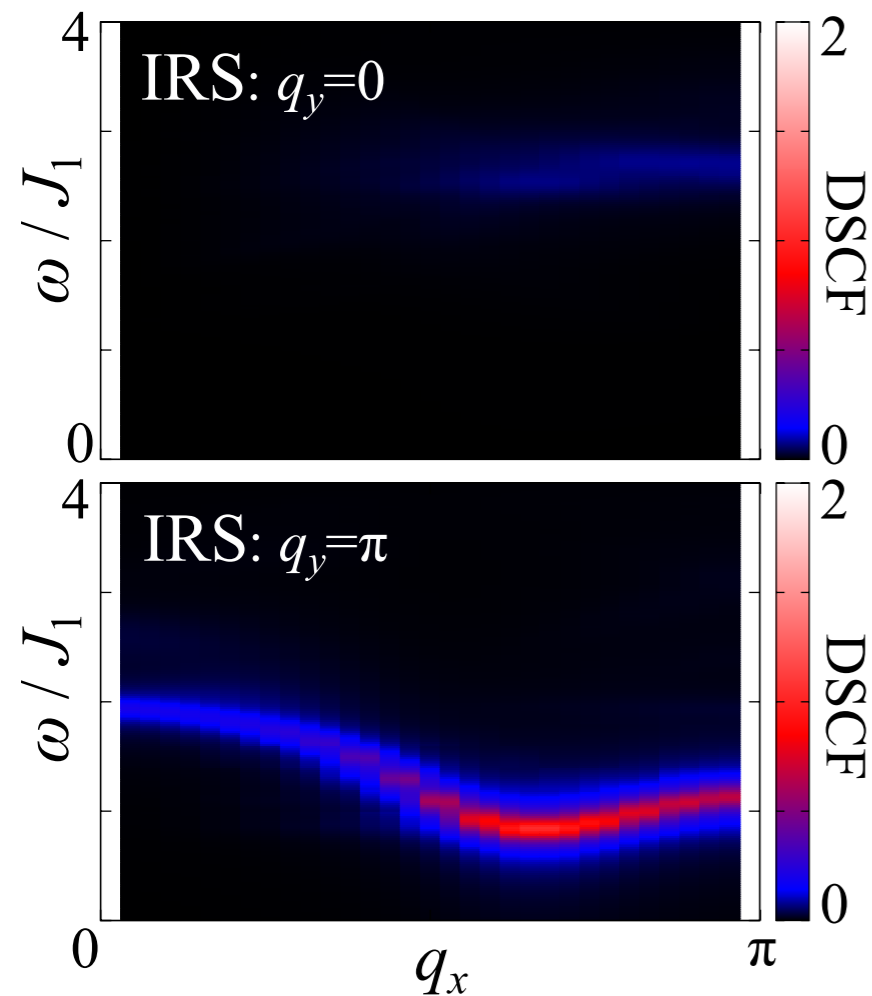
# Result: Frustration Effects

DSCF in Incomm. RS phase:



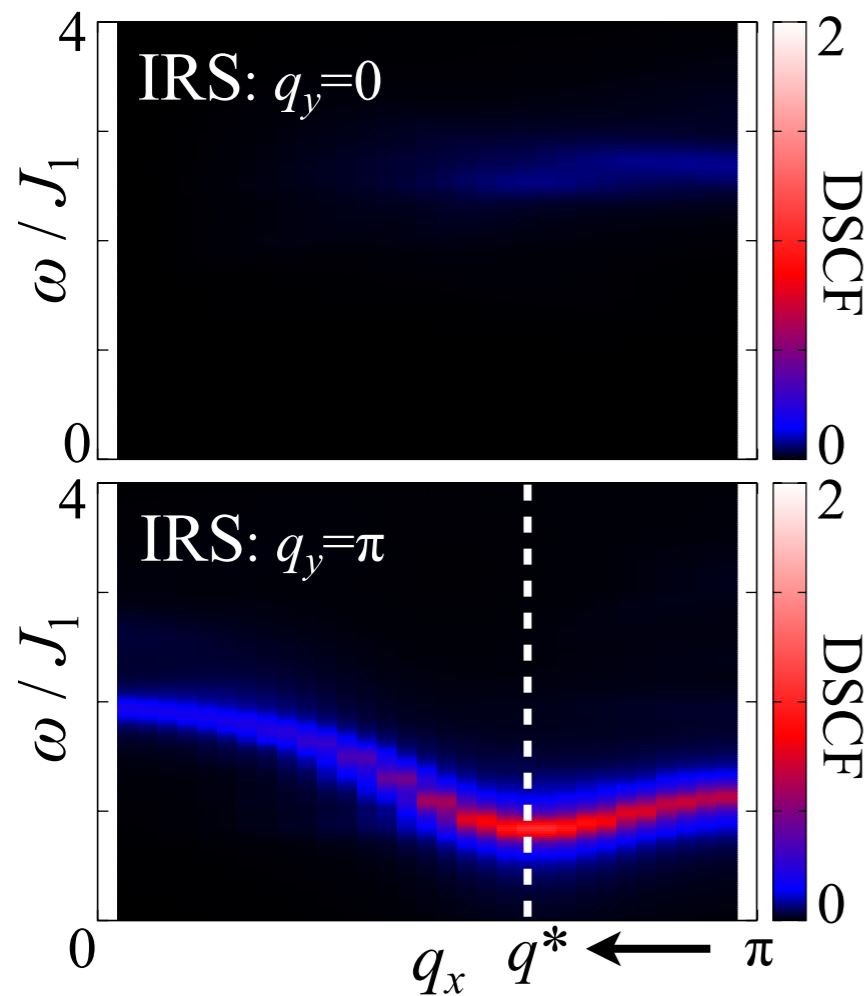
# Result: Frustration Effects

DSCF in Incomm. RS phase:



# Result: Frustration Effects

DSCF in Incomm. RS phase:

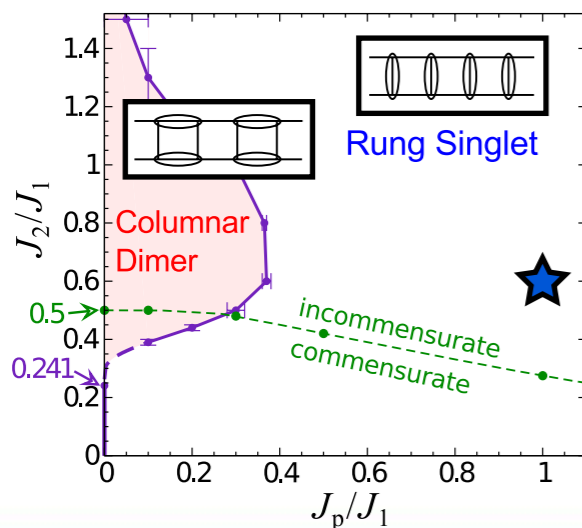


Strong rung-coupling limit ( $J_1, J_2 \ll J_p$ )

$$\epsilon_T(q_x) \cong J_p + J_1 \cos(q_x) + J_2 \cos(2q_x) + \frac{3}{4} \left( \frac{J_1^2}{J_p} + \frac{J_2^2}{J_p} \right)$$

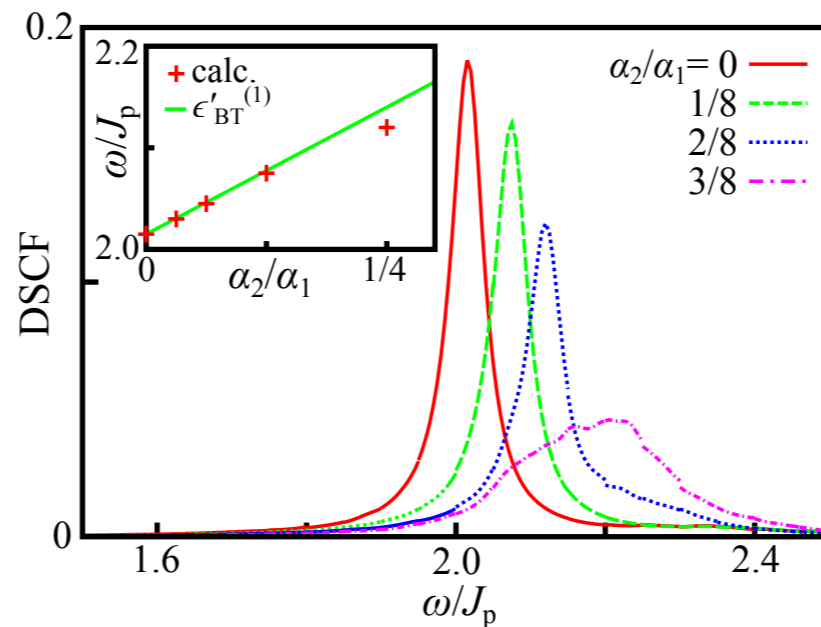
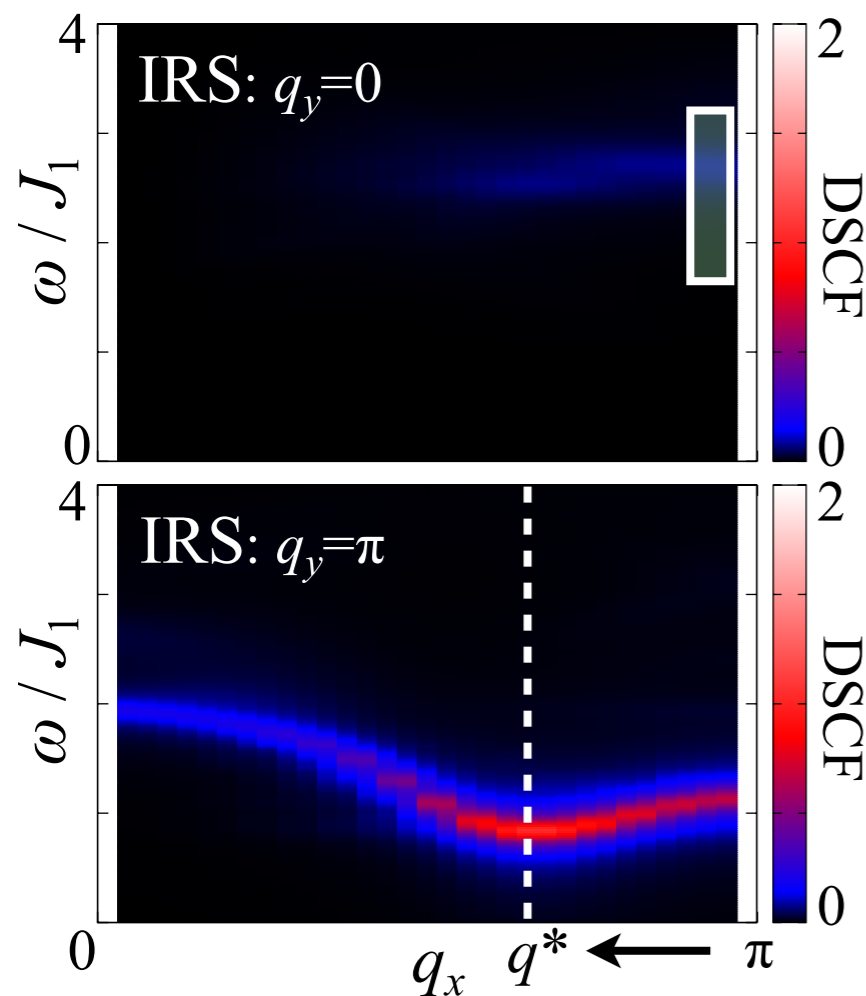
$$q^* \cong \cos^{-1} \left( -\frac{J_1}{4J_2} \right)$$

➡ Frustration affects the wave number of the lowest excitation, and change it from  $\pi$  to incommensurate one.



# Result: Frustration Effects

DSCF in Incomm. RS phase:



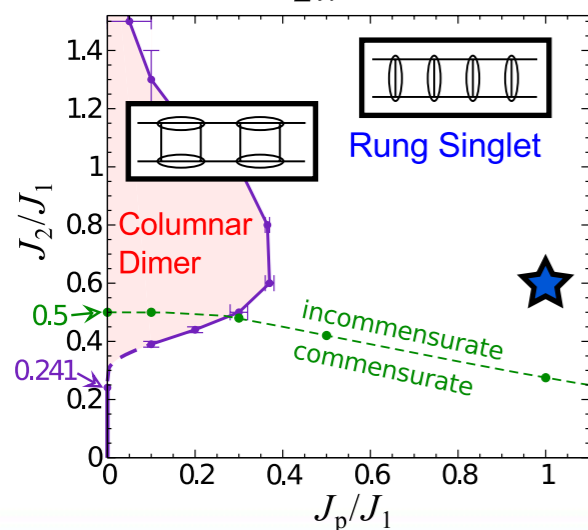
With large frustration, the bound triplon is smeared over the continuum.

Strong rung-coupling limit ( $J_1, J_2 \ll J_p$ )

$$\epsilon_T(q_x) \cong J_p + J_1 \cos(q_x) + J_2 \cos(2q_x) + \frac{3}{4} \left( \frac{J_1^2}{J_p} + \frac{J_2^2}{J_p} \right)$$

$$q^* \cong \cos^{-1} \left( -\frac{J_1}{4J_2} \right)$$

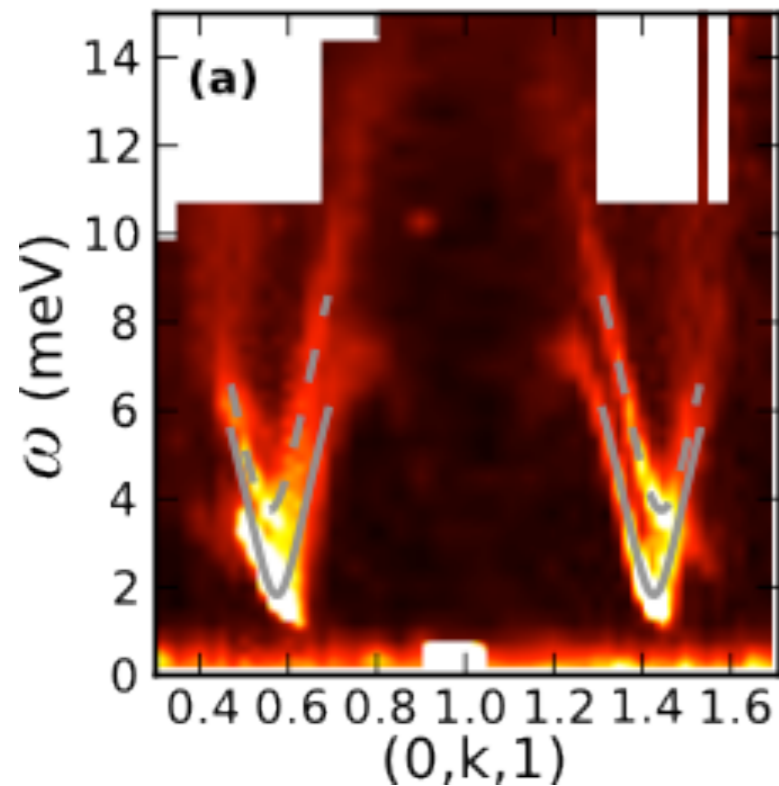
Frustration affects the wave number of the lowest excitation, and change it from  $\pi$  to incommensurate one.



# Experiment: inelastic neutron scattering

Grand-state phase:

Inelastic neutron scattering for  $\text{BiCu}_2\text{PO}_6$



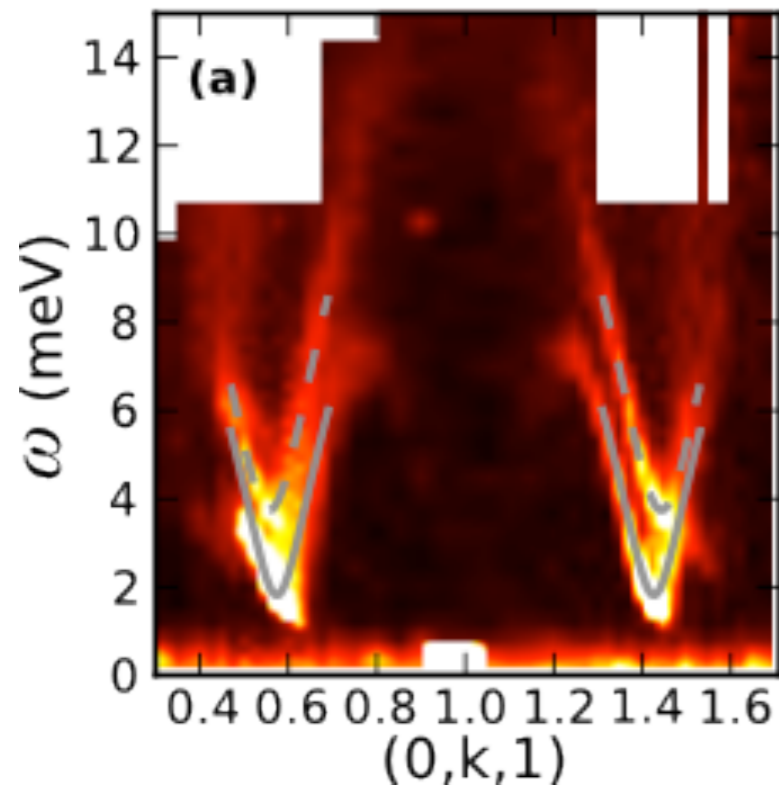
Triplon excitation with an incomm. wave number is observed.

K.W. Plumb, *et al*, arXiv:1301.5324.

# Experiment: inelastic neutron scattering

## Grand-state phase:

### Inelastic neutron scattering for $\text{BiCu}_2\text{PO}_6$



K.W. Plumb, *et al.*, arXiv:1301.5324.

Triplon excitation with an incomm. wave number is observed.

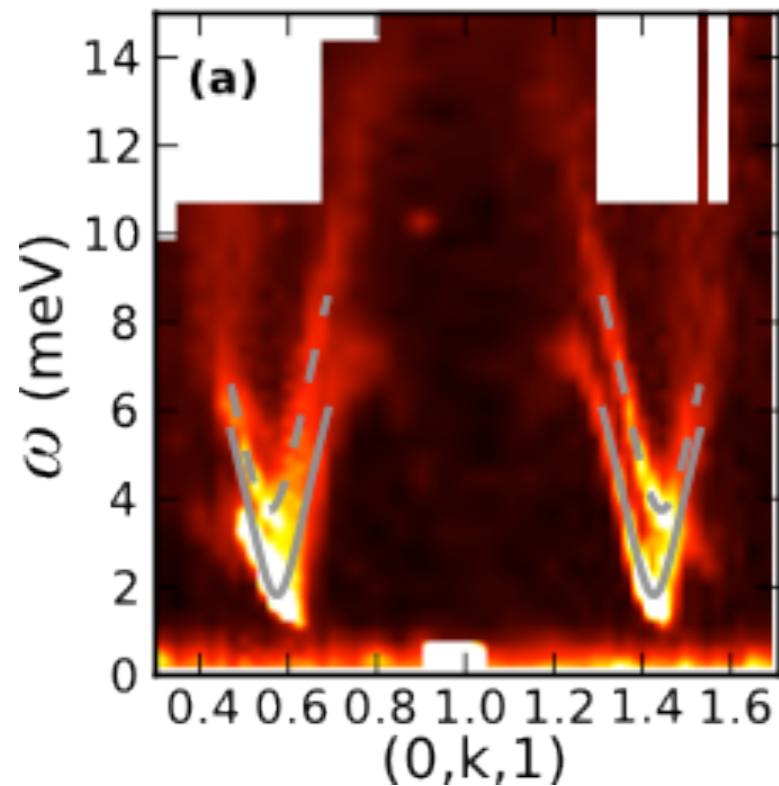
- $\text{BiCu}_2\text{PO}_6$  is located in the incomm. rung-singlet phase.
- The triplon dispersion relation indicates comparable magnitudes of exchange energies,  $J_1 \sim J_2 \sim J_p$ .



# Experiment: inelastic neutron scattering

## Grand-state phase:

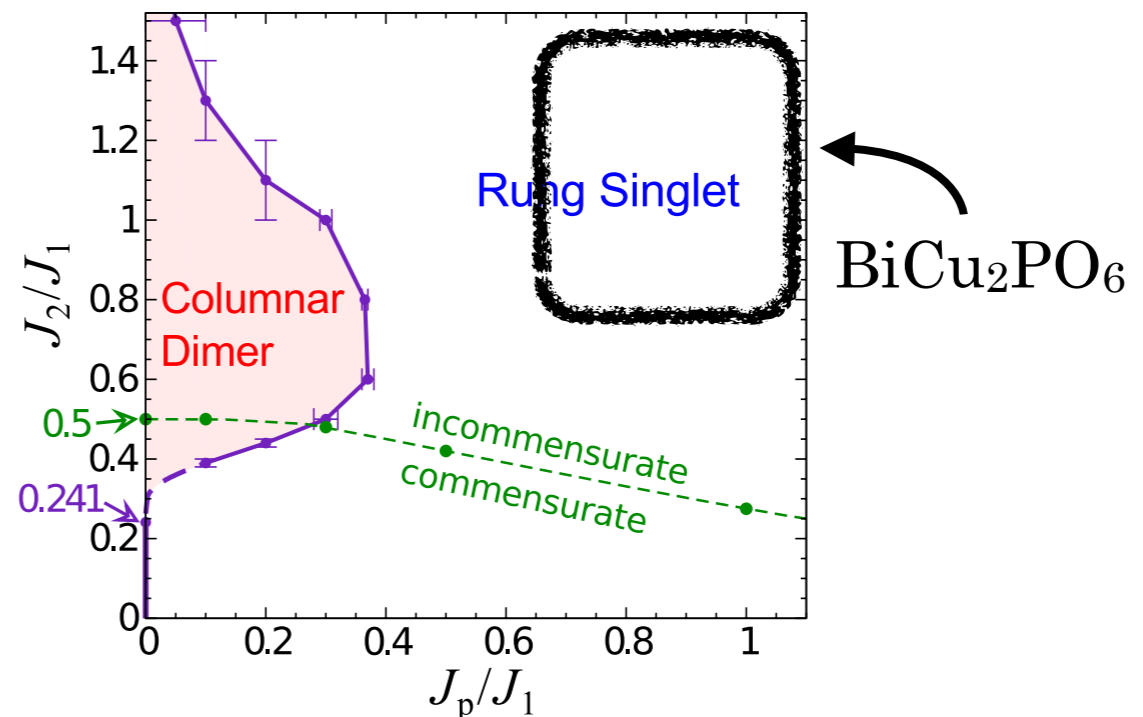
### Inelastic neutron scattering for $\text{BiCu}_2\text{PO}_6$



K.W. Plumb, *et al*, arXiv:1301.5324.

Triplon excitation with an incomm. wave number is observed.

- $\text{BiCu}_2\text{PO}_6$  is located in the incomm. rung-singlet phase.
- The triplon dispersion relation indicates comparable magnitudes of exchange energies,  $J_1 \sim J_2 \sim J_p$ .



A. Lavarélo, *et al*, PRB 84, 144407 (2011).

# Field effect

## Frustrated two-leg spin ladder

$$\begin{aligned}\mathcal{H} &= \mathcal{H}_1 + \mathcal{H}_2 + \mathcal{H}_p + \mathcal{H}_Z \\ \mathcal{H}_1 &= J_1 \sum_j \left[ \mathbf{S}_{j,u} \cdot \mathbf{S}_{j+1,u} + \mathbf{S}_{j,l} \cdot \mathbf{S}_{j+1,l} \right] \\ \mathcal{H}_2 &= J_2 \sum_j \left[ \mathbf{S}_{j,u} \cdot \mathbf{S}_{j+2,u} + \mathbf{S}_{j,l} \cdot \mathbf{S}_{j+2,l} \right] \\ \mathcal{H}_p &= J_p \sum_j \mathbf{S}_{j,u} \cdot \mathbf{S}_{j,l} \\ \mathcal{H}_Z &= h^z \sum_j (S_{j,u}^z + S_{j,l}^z)\end{aligned}$$

## Non-interacting triplon (NIT)

$$\begin{aligned}\mathcal{H}_{\text{eff}} &= \sum_{q,\alpha} \omega(q) n_q^\alpha + \text{sgn}(\alpha) h^z n_q^\alpha \\ \omega(q) &= J_1 \cos(q) + J_2 \cos(2q) + J_p \\ n^\alpha &= t^{\alpha\dagger} t^\alpha \quad (\alpha = +, 0, -)\end{aligned}$$

- ☛ Triplon is a hard-core boson.
- ☛ Bose-Einstein condensation is expected induced by magnetic field.



Bond-operator transform & Mean-field approx.

$$\begin{aligned}s_j^\dagger |0\rangle &= |s\rangle_j = \frac{1}{\sqrt{2}} (|\uparrow\rangle_{j,u} |\downarrow\rangle_{j,l} - |\downarrow\rangle_{j,u} |\uparrow\rangle_{j,l}) \\ t_j^{+\dagger} |0\rangle &= |t^+\rangle_j = |\uparrow\rangle_{j,u} |\uparrow\rangle_{j,l} \\ t_j^{0\dagger} |0\rangle &= |t^0\rangle_j = \frac{1}{\sqrt{2}} (|\uparrow\rangle_{j,u} |\downarrow\rangle_{j,l} + |\downarrow\rangle_{j,u} |\uparrow\rangle_{j,l}) \\ t_j^{-\dagger} |0\rangle &= |t^-\rangle_j = |\downarrow\rangle_{j,u} |\downarrow\rangle_{j,l}\end{aligned}$$



# Bose-Einstein condensation

## Non-interacting triplon (NIT)

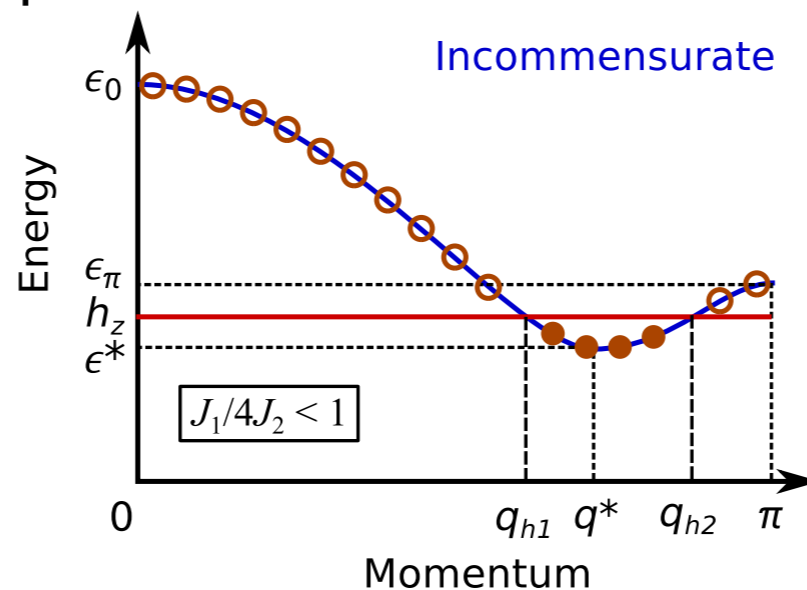
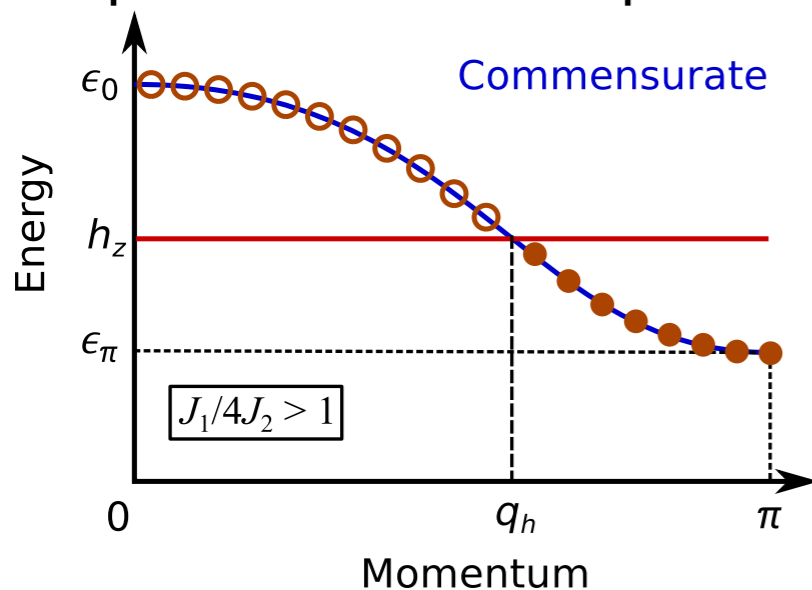
$$\mathcal{H}_{\text{eff}}^{(-)} = \sum_q \omega(q) n_q^- - h^z n_q^-$$

$$\omega(q) = J_1 \cos(q) + J_2 \cos(2q) + J_p$$

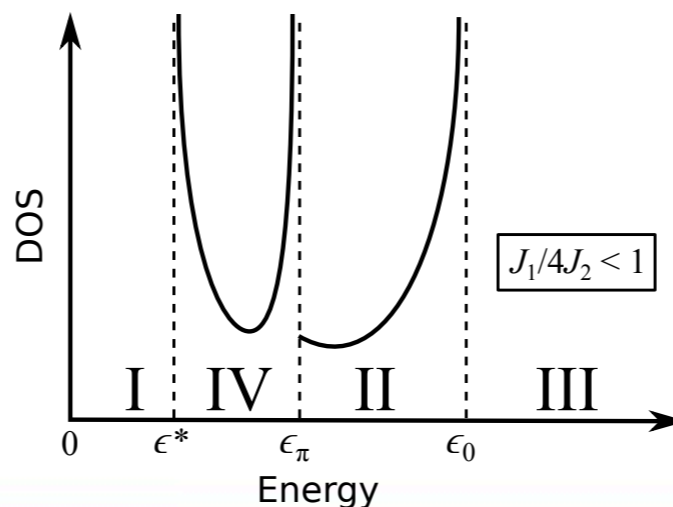
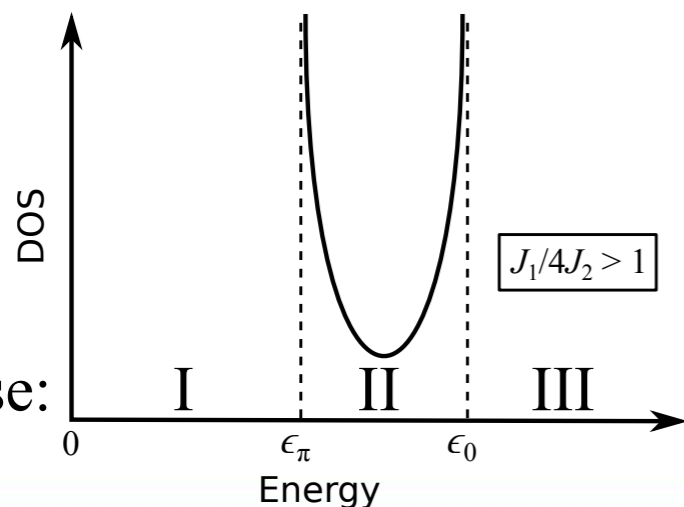
## Bose-Einstein condensation

Bose gas	NIT
boson particle	triplon
boson num. ( $N$ )	magnetization ( $M$ )
chem. potential ( $\mu$ )	magnetic field ( $h^z$ )

## Dispersion relation & triplon occupation



## Density of states



Without frustration, there are three phases:

Phase I:  $h^z < \epsilon_\pi$ ,  $M = 0$ , gapped.

Phase II:  $\epsilon_\pi < h^z < \epsilon_0$ ,  $0 < M < 1$ , gapless.

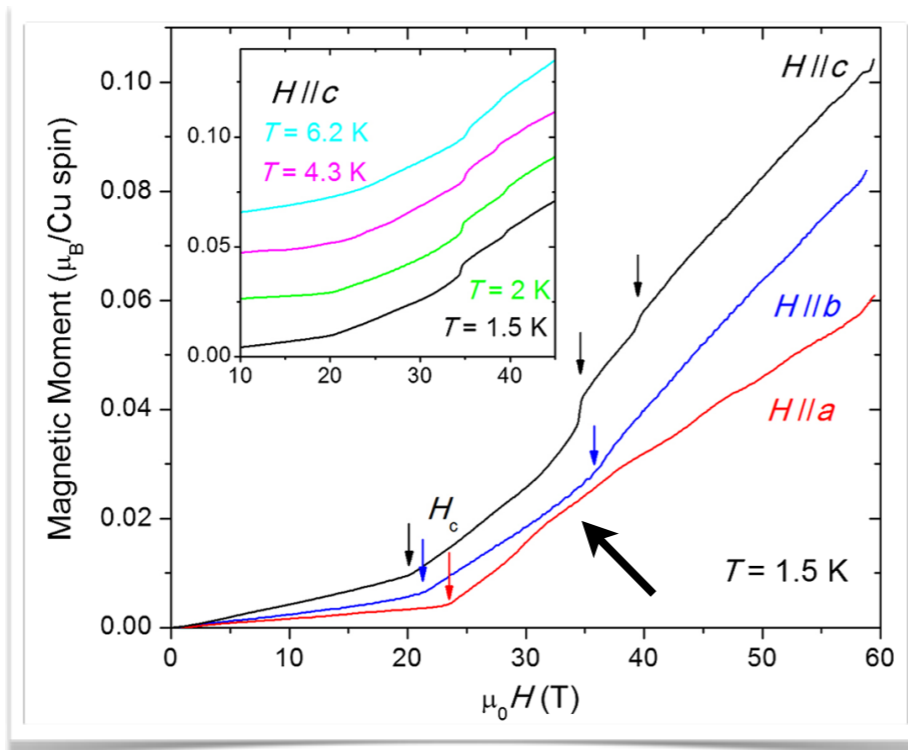
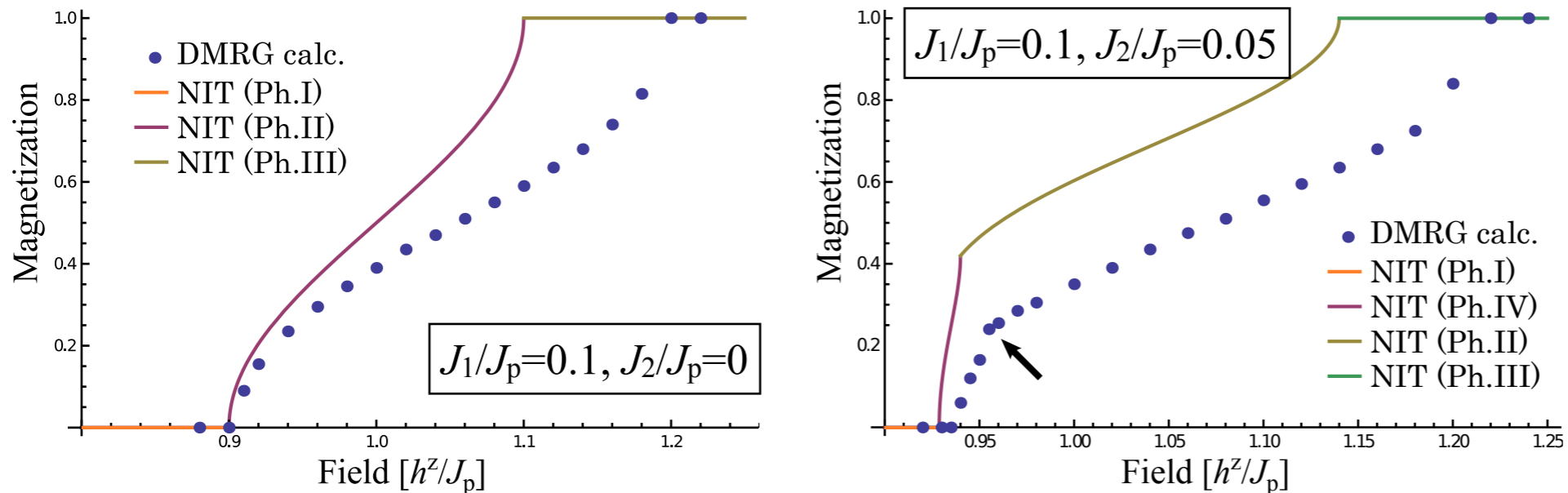
Phase III:  $\epsilon_0 < h^z$ ,  $M = 1$ , gapped.

With frustration, a new gapless phase appears,

Phase IV:  $\epsilon^* < h^z < \epsilon_\pi$ ,  $0 < M < 1$ , gapless.

# M-H curve

## M-H curve



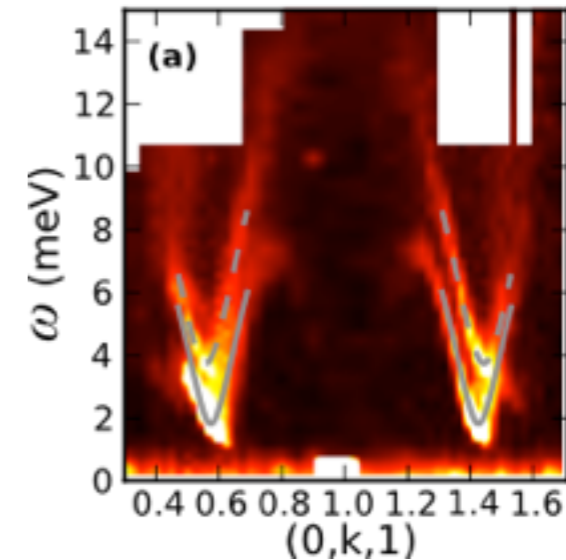
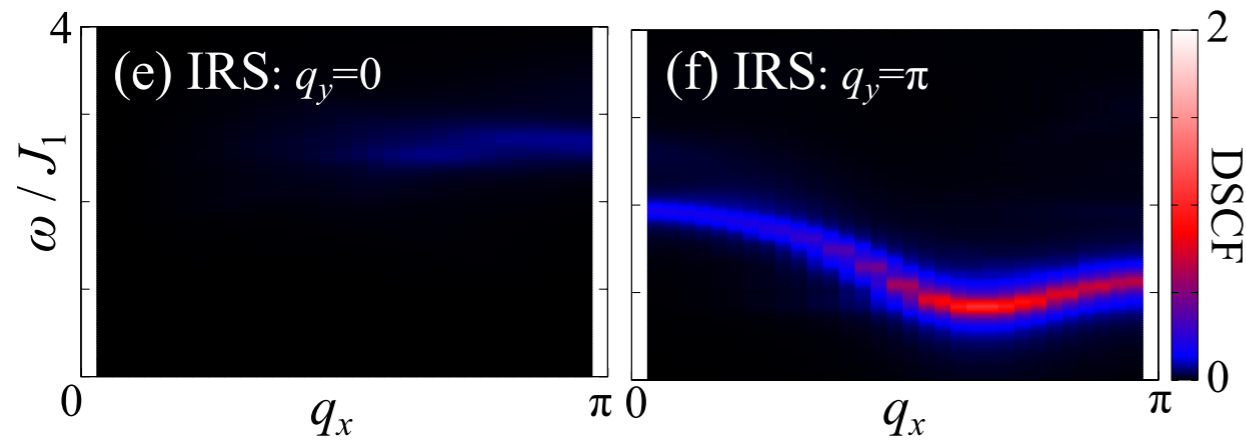
Y. Kohama, *et al*, PRL **109**, 167204 (2012).

With frustration, the cusp-like singularity appears in M-H curve.

The phase transition in the compound  $\text{BiCu}_2\text{PO}_6$  can be understood using triplon picture with frustration.

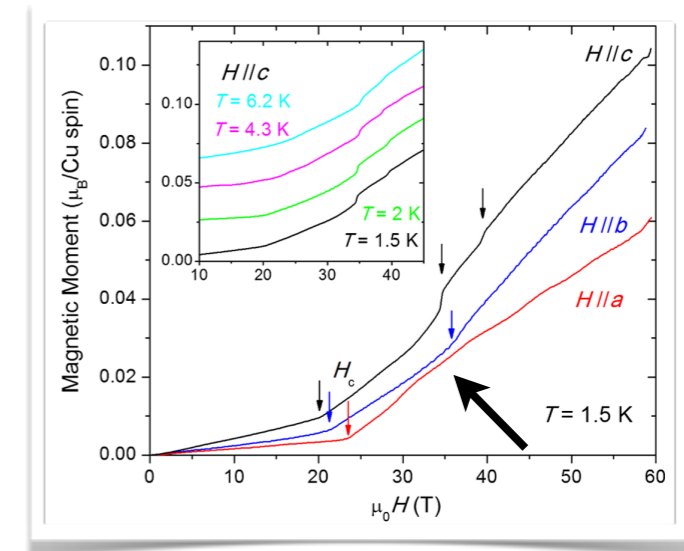
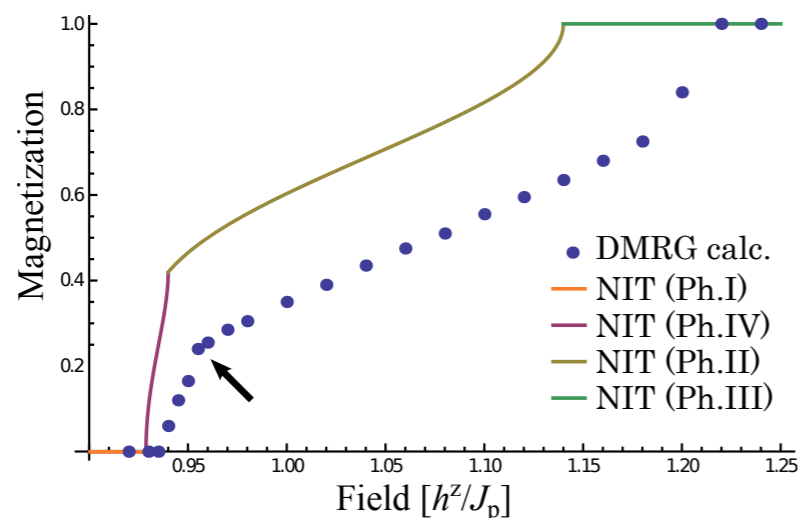
# Summary

We determine the ground-state phase of  $\text{BiCu}_2\text{PO}_6$ , with excitation spectra obtained by DDMRG calculation and INS experiment.



K.W. Plumb, *et al*, arXiv:1301.5324.

We clarify the phase transition in  $\text{BiCu}_2\text{PO}_6$ , with M-H curve of DMRG calculation, non-interacting triplon analysis, and the experiment.

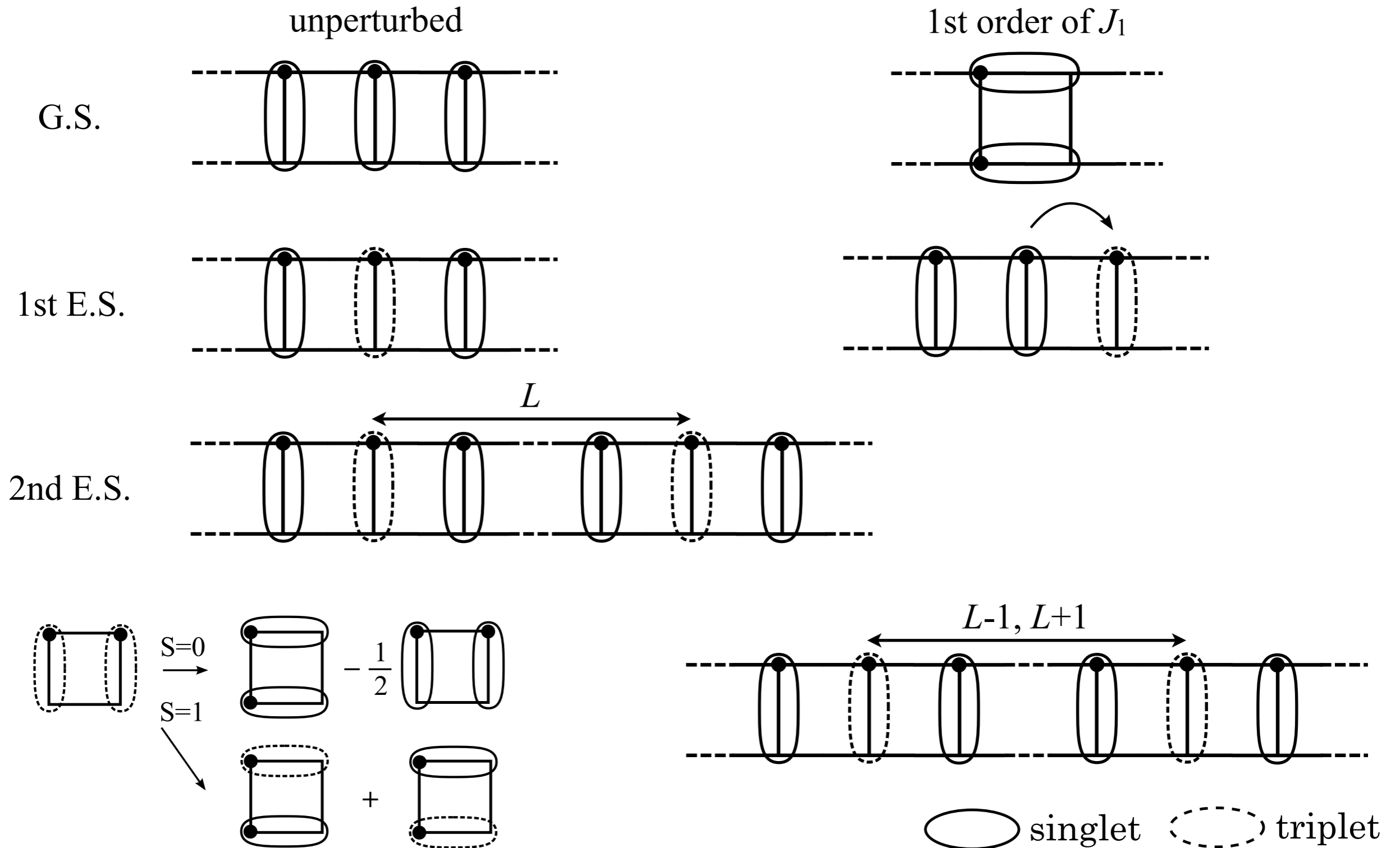


Y. Kohama, *et al*, PRL **109**, 167204 (2012).

# Appendix

# Purbation analysis

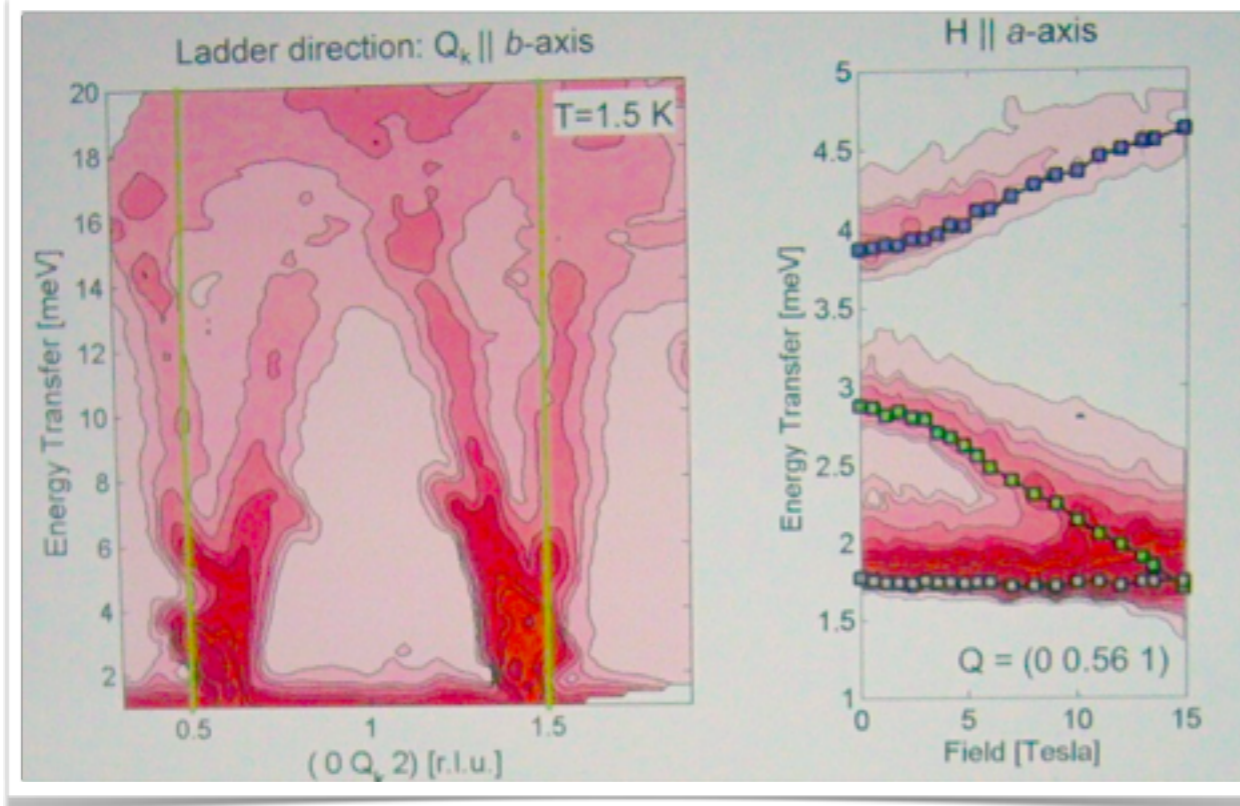
## Strong rung-coupling limit





# Zeeman splitting

- ◆ Field dependence (experiment) ref. ICM poster



➡ Field effects on lowest excitations seems Zeeman splitting of triplet.

- ◆ 2 spins Hamiltonian with anisotropy

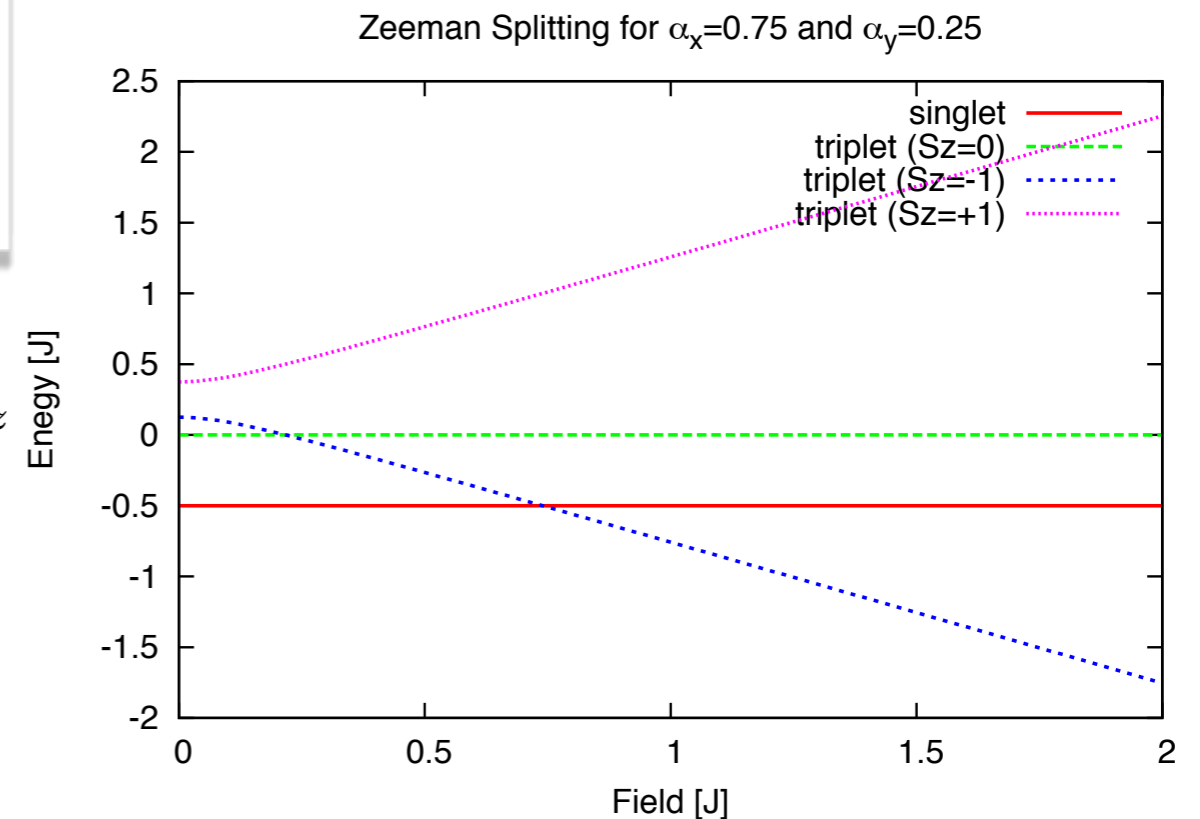
$$\mathcal{H} = J(\alpha_x S_1^x S_2^x + \alpha_y S_1^y S_2^y + S_1^z S_2^z) + (S_1^z + S_2^z)H_z$$

$$E^s = -\frac{J}{4} (1 + |\alpha_x + \alpha_y|),$$

$$E_0^t = \frac{J}{4} (-1 + |\alpha_x + \alpha_y|),$$

$$E_{-1}^t = \frac{J}{4} \left[ 1 - \sqrt{\frac{16H_z^2}{J^2} + (\alpha_x - \alpha_y)^2} \right],$$

$$E_1^t = \frac{J}{4} \left[ 1 + \sqrt{\frac{16H_z^2}{J^2} + (\alpha_x - \alpha_y)^2} \right].$$

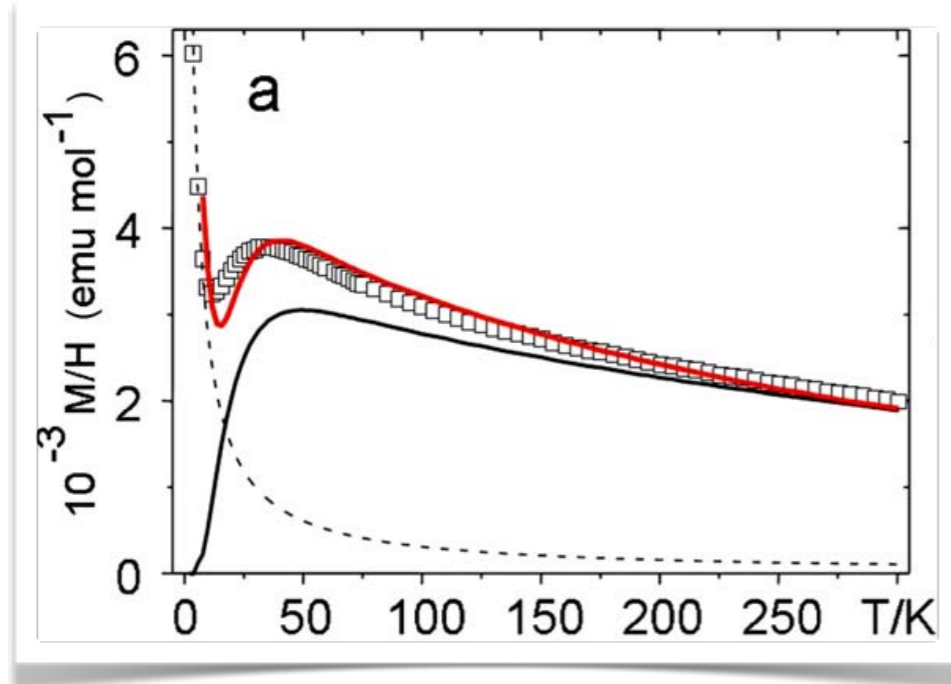


➡ Spin interaction between two spins forming triplet has anisotropy.



# Real compound

## ◆ Susceptibility



➤ Fitting (paramag. impurity + frustrated ladder) gives better coincidence, than fitting by using the ladder model.

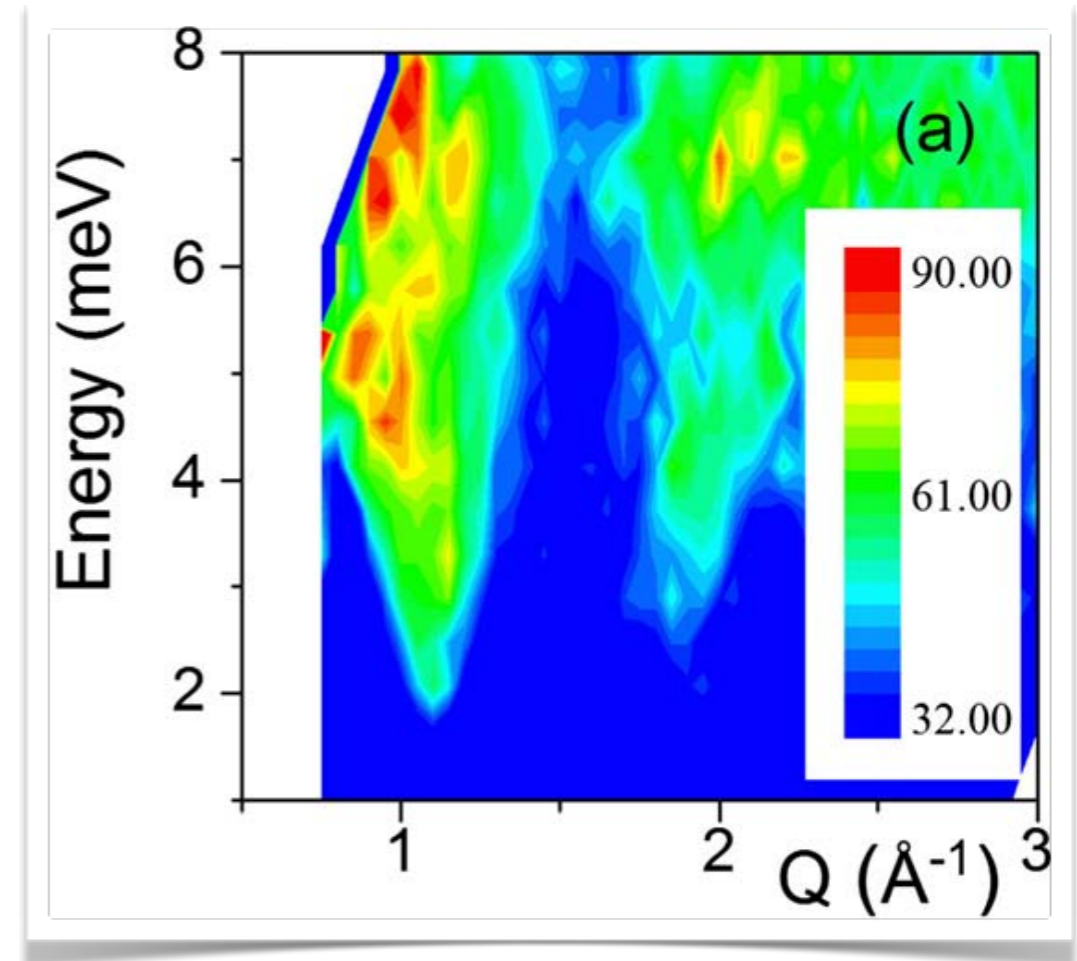
Here, fitting function is as follows,

$$\chi_{\text{fit}}(T) = C/T + \chi_{1-2-4}(T).$$

$$\rightarrow J_1/k_B = 137 \text{ K}, J_2/k_B = 73 \text{ K}, J_4/k_B = 58 \text{ K}.$$

➤ Experimental results are consistent for the  $J_1$ - $J_2$ - $J_4$  model, but exchange ratios  $J_2/J_1$  &  $J_4/J_1$  are not determined precisely.

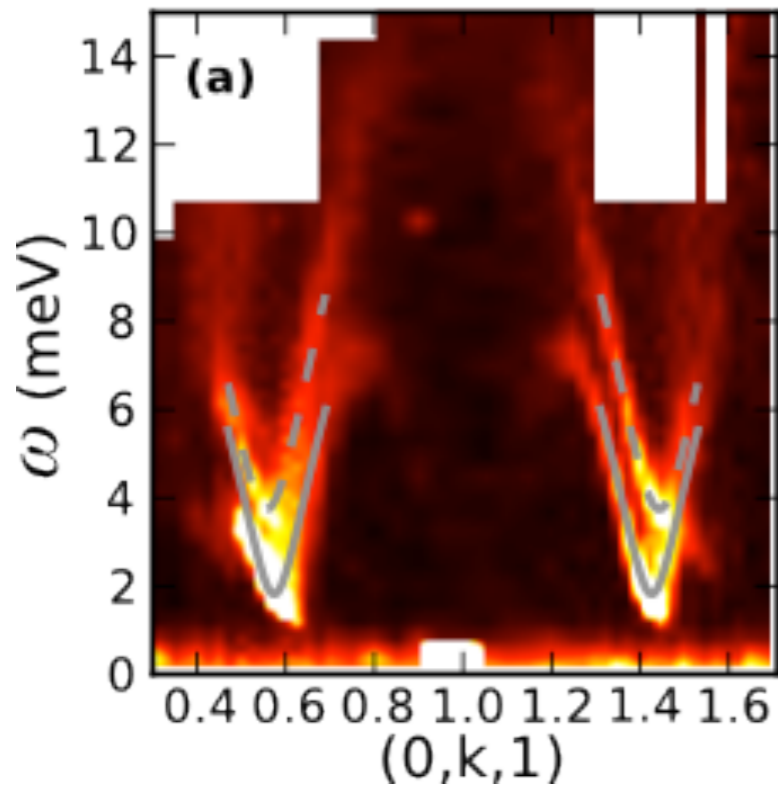
## ◆ Inelastic neutron scattering for powder



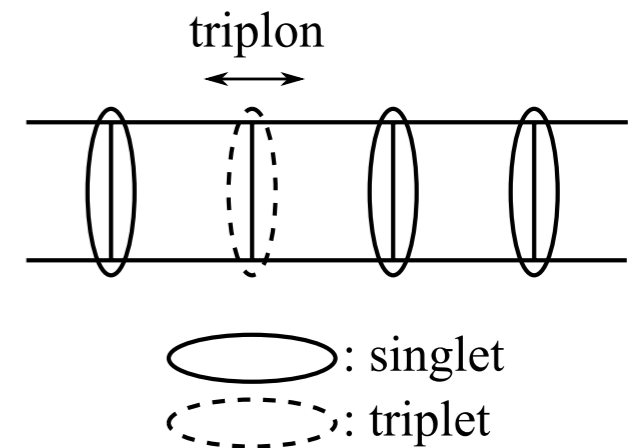
➤ Inelastic Neutron scattering is done for powder sample. The gap is estimated at 4 meV (46 K).

O. Mentré, *et al*, PRB 80, 180413(R) (2009).

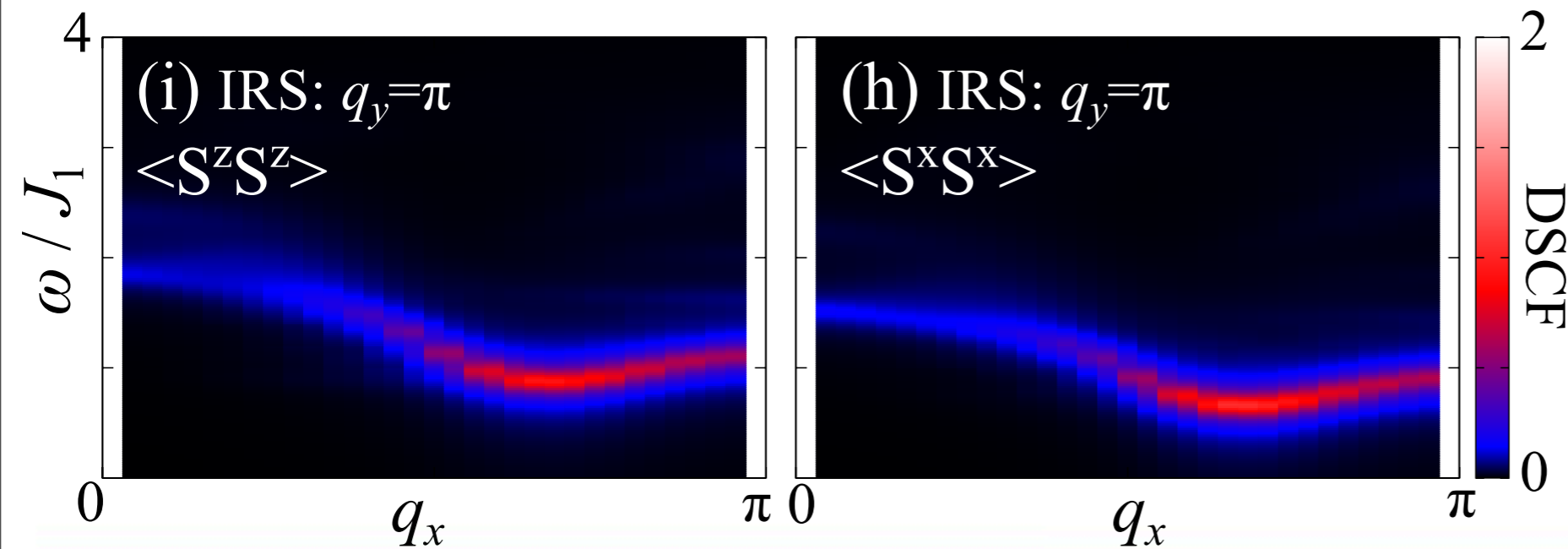
# Inelastic neutron scattering



→ Splitting of triplon mode



K.W. Plumb, *et al*, arXiv:1301.5324.



$$E^s = -\frac{J}{4} (1 + 2|\alpha_{\text{Ising}}|),$$

$$E_0^t = \frac{J}{4} (-1 + 2|\alpha_{\text{Ising}}|),$$

$$E_{-1}^t = \frac{J}{4} \left[ 1 - \left| \frac{4H_z}{J} \right| \right],$$

$$E_1^t = \frac{J}{4} \left[ 1 + \left| \frac{4H_z}{J} \right| \right].$$